Hydrol. Earth Syst. Sci. Discuss., 12, 3527–3592, 2015
www.hydrol-earth-syst-sci-discuss.net/12/3527/2015/
doi:10.5194/hessd-12-3527-2015

Hydrology and Earth System Sciences
Discussions
Open Access

Predicting land use and soil controls on erosion and sediment redistribution in agricultural loess areas: model development and cross scale verification

U. Scherer[1,*] and E. Zehe[1]

[1]Institute for Water and River Basin Management, Chair of Hydrology, Karlsruhe Institute of Technology, Karlsruhe, Germany
[*]now at: Karlsruhe Institute of Technology, Energy and Environment Programs, Karlsruhe, Germany

Received: 27 February 2015 – Accepted: 4 March 2015 – Published: 31 March 2015

Correspondence to: U. Scherer (ulrike.scherer@kit.edu)

Published by Copernicus Publications on behalf of the European Geosciences Union.

Abstract

This study quantifies soil and land use controls on sediment mobilisation and redistribution in cultivated loess soil landscapes, as these landscapes are frequently used for intensive cultivation and are highly susceptible to erosion. To this end we developed and verified a process based model named CATFLOW-SED at the plot, hillslope and catchment scales. The model relies on an explicit representation of hillslopes and their dominant physiographical characteristics which control overland flow formation, particle detachment and sediment redistribution (transport and sedimentation). Erosion processes are represented by means of the steady state approximation of the sediment continuity equation, their interaction is conceptualized based on the sediment transport capacity of overland flow. Particle detachment is represented by means of a threshold approach accounting for the attacking forces of rainfall and overland flow which need to exceed a threshold in soil erosion resistance to mobilize soil particles (Scherer et al., 2012). Transport capacity of overland flow is represented as proposed by Engelund and Hansen (1967). Top soil particles and aggregates are detached and transported according to their share in the particle size distribution. Size selective deposition of soil particles is determined based on the sink velocity of the various particle size classes. CATFLOW-SED was verified on the plot, hillslope and catchment scale, where either particle detachment or lateral redistribution or sedimentation is the limiting factor, to check whether the respective parameterizations are transferable for simulations at the next higher scale. For verification we used the Weiherbach data set providing plot scale rainfall simulation experiments, long term monitoring of sediment yields on a selected hillslope as well as observed sediment fluxes at the catchment outlet. Our findings corroborate that CATFLOW-SED predicted the sediment loads at all scales within the error margin of the measurements. An accurate prediction of overland flow turned out as being necessary and sufficient to guarantee spatial transferability of erosion parameters optimized at smaller scales to the next higher scale without need for further calibration.

HESSD

12, 3527–3592, 2015

Based on the verified model setup, we investigate the efficiency of land use management to mitigate measures in erosion scenarios for cultivated loess landscapes.

1 Introduction

Surface runoff, erosion and sediment redistribution play a pivotal role in the terrestrial ecosystem as they directly influence water quality, soil biogeochemical cycles and soil functions. In particular, surface waters in intensively cultivated areas are threatened by emissions of sediments and associated nutrients and contaminants (Owens et al., 2005; Walling, 2006; Kronvang et al., 2007; Bilotta and Brazier, 2008; Verheijen et al., 2009). There is thus an urgent need for adequate models to support design of mitigation measures to prevent on- and off-site damages of soil erosion as well as to estimate global change impacts on erosion and related environmental damage.

Soil erosion results from non-linear interactions of three main processes with different characteristic spatial scales, namely detachment, transport and deposition of sediments. Particles and aggregates are eroded when local thresholds for surface runoff generation and particle detachment are exceeded. These thresholds depend on topography, patterns of soil types, land use and management practice (Zhang et al., 2009b; Knapen et al., 2007; Scherer et al., 2012). The most important temporally varying controls on surface runoff formation and erosion are precipitation intensity, antecedent soil moisture as well as surface density and connectivity of vertical preferential flow paths (Zehe and Sivapalan, 2009; Zehe and Blöschl, 2004). The latter are either biologically mediated as in the case of worm borrows, root channels or emerge in the case of shrinkage cracks during sufficiently dry soil moisture conditions (Zehe et al., 2007).

The ratio of eroded sediment which is delivered to surface water bodies depends however on the transport capacity of overland flow and its limiting factors, as well as on the spatial connectivity of overland flow paths to the river network. Hillslope scale patterns of topography, morphology, land use and vegetation are thus first order controls of sediment delivery (Cammeraat, 2004; Wainwright et al., 2011; Lesschen et al.,

HESSD
12, 3527–3592, 2015

2009) as they control overland flow depth and velocity and thereby sediment transport capacity. A decreasing slope at the hill foot or an increasing surface roughness due to vegetation cover reduces for instance overland flow velocity: soil particles and aggregates are deposited and thus retained within the catchment (Beuselinck et al., 2000; Takken et al., 1999).

The main asset of process-based numerical models is that, in principle, they may represent these cross scale process interactions, predict water and sediment dynamics at hillslopes and small catchment scales and even project related global change impacts. However, most process-based erosion models rely in fact on a mixture of first principles and empirical parameterizations of, for instance, particle detachment and transport capacity. The "zoo" of erosion models that have been developed in recent years thus differ significantly with respect to (a) process representation and their empirical parameterization, (b) the spatial and temporal scales addressed by the models' scope and (c) last not least the underlying numerical methods (Harmon and Doe, 2001; Boardman and Favis-Mortlock, 1998; Jetten and Favis-Mortlock, 2006). The present state of the art is thus far away from the above sketched ideal of universally applicable models and transferable model parameterizations (Morgan and Quinton, 2001; Boardman, 2006). The large spatial and temporal variability of soil erosion phenomena and of the underlying landsape controls cause, furthermore, a considerable uncertainty in the model parameters. This strongly hampers calibration and validation of spatially distributed models (Jetten et al., 2003; Nearing, 2006; Brazier et al., 2001, 2000; Morgan and Quinton, 2001).

Here we suggest that these problems cannot be solved by constructing ever more complicated models. The challenge is to balance the necessarymodel complexity to resolve the dominant process patterns and related landscape characteristics with greatest possible simplicity to avoid model over-parameterization and related problems (Paik and Kumar, 2010; Zehe and Sivapalan, 2009; Jetten et al., 2003). Our notion of a balanced model complexity is based on the following essential model requirements:

1. The model should predict the interplay of water driven mobilization, redistribution and export of sediments from catchments for the key different grain size fractions in the soil landscape of interest. This implies that spatial variability of the underlying controls must be explicitly addressed and the hillslope catena is the key organizing landscape element (Jackisch et al., 2014).

2. The model should be based on observable parameters and the representations of the main processes should be testable in an independent manner along the hierarchy of characteristic spatial scales of the governing processes; this avoids parameter interdependence, which reduces their identifiability and is a major source of predictive/extrapolative model uncertainty.

3. The model should be capable of estimating catchment scale impacts of land use and climate change within spatially explicit and continuous simulations.

In the present study we demonstrate the development and verification of such a balanced model for loess landscapes, as these are highly susceptible to erosion and are frequently used for intensive cultivation (Clemens and Stahr, 1994; Van Oost et al., 2005; Zhang et al., 2009b; Rejman and Iglik, 2010; Winteraeken and Spaan, 2010). As reliable spatially distributed representation of the various runoff processes along the catena is of prime importance for process-based erosion modelling, we chose CATFLOW as a model platform for supplementing the components for erosion and named the extended model CATFLOW-SED. This is because CATFLOW is a catena based dynamic, spatially distributed model system that was successfully applied to predict runoff formation, the water balance and solute transport in different landscapes and at different scales (Maurer, 1997; Plate and Zehe, 2008; Zehe et al., 2001, 2005; Zehe and Blöschl, 2004; Graeff et al., 2009; Klaus and Zehe, 2010, 2011; Wienhöfer and Zehe, 2014).

In the remaining sections we discuss the dominant controls of erosion and deposition processes in loess landscapes and suggest process approaches of adequate complexity. We then explain their implementation into the hydrological model as well as their

HESSD
12, 3527–3592, 2015

evaluation against observations at the plot, hillslope and catchment scales in a typical representative of a loess soil landscape. Finally, we discuss the sensitivity of the most important model parameters and evaluate the capability of the model to project change impacts exemplified by the simulation of different land use patterns

2 Theory, model structure and numerics

2.1 Process approaches for erosion and their parameterizations

2.1.1 The sediment continuity equation and interactions of different processes

The principle of mass conservation in the form of the sediment continuity equation (Eq. 1) is fundamental for representing and coupling different erosion processes. As proposed by Bennett (1974) it consists of three terms: the first one represents the divergence of the solid flux along the flow path, the second accounts for changes in sediment storage in the cross-section and the third term accounts for detachment and deposition and related changes of local bed elevation. These three terms are equal to the dispersion of suspended solids.

$$\frac{\partial\left(h\cdot v_\mathrm{p}\cdot c_\mathrm{v}\right)}{\partial x}+\frac{\partial\left(c_\mathrm{v}\cdot h\right)}{\partial t}+(1-n)\cdot\frac{\partial y}{\partial t}=\frac{\partial}{\partial x}\left(h\cdot\varepsilon_\mathrm{p}\cdot\frac{\partial c_\mathrm{v}}{\partial x}\right) \tag{1}$$

where h is flow depth in m, v_p velocity of sediment in $\mathrm{m\,s^{-1}}$, c_v volume concentration of sediment in $\mathrm{m^3\,m^{-3}}$, x spatial coordinate in m, t time step in s, n porosity of deposited sediment, y change of local bed elevation and ε_p sediment particle mass transfer coefficient in $\mathrm{m^2\,s^{-1}}$.

Dispersion is normally negligible in hillslope erosion processes (Bennett, 1974) when compared to the other processes. Also the storage term can be neglected for small and slowly changing overland flow depths (Haan et al., 1994). Both simplifications lead to the stationary form of the sediment continuity equation (Eq. 2), which was implemented in CATFLOW-SED. We thus approximate temporal changes of erosion and deposition rates by a sequence of steady state conditions.

$$\frac{\partial q_s}{\partial x} = \Phi(x,t) \tag{2}$$

where q_s is sediment mass flow per unit width in $\mathrm{kg\,m^{-1}\,s^{-1}}$, Φ net input/output of sediments from overland flow in $\mathrm{kg\,m^{-2}\,s^{-1}}$, x length coordinate in m and t time step in s.

The term $\Phi(x,t)$ in Eq. (2) quantifies the net erosion and deposition rates and is thus controlled by the interaction of detachment, transport and deposition of sediments. In line with many process-based erosion models such as CREAMS (Knisel, 1980), WEPP (USDA, 2015), LISEM (De Roo et al., 1998), EUROSEM (Morgan et al., 1998), ANSWERS (Bouraoui and Dillaha, 1996) we determine, on the basis of available transport capacity, whether soil particles are detached or deposited.

Meyer and Wischmeier (1969) suggested that detachment of soil particles and aggregates is a separable process and, after the threshold value for soil detachment is exceeded, the detachment rate increases linearly until the transport capacity is reached. In contrary to this approach, Foster and Meyer (1972, 1975) proposed that the detachment rate depends on the difference between the transport capacity T_c ($\mathrm{kg\,m^{-1}\,s^{-1}}$) and the actual sediment load (Eq. 3). This implies a downstream/downslope decrease in the detachment rate, as the sediment concentration increases downstream. Please note that this approach is mathematically equivalent to a first-order reaction (Merten et al., 2001; Huang et al., 1996; Govers et al., 2007).

$$\frac{\partial q_s}{\partial x} = a \cdot (T_c - q_s) \tag{3}$$

where a is rate control constant in $\mathrm{m^{-1}}$.

This equivalence implies, as criticized by Nearing et al. (1990), that Foster and Meyer (1972, 1975) postulated a linear relation between the two boundary points of a discrete model element along the flow path without any experimental verification. In fact the change in the transport deficit is deemed as being proportional to the deficit itself. The relationship between both points is, however, discussed controversially in the literature (Govers et al., 2007). Huang et al. (1996) observed during field experiments that detachment in rills and sediment transport appeared to be de-coupled; their experimental data support the concept of Meyer and Wischmeier (1969). In line with this, Giménez and Govers (2002) report that sediment load had no systematic effect on the detachment rate in their laboratory experiments. On the other hand, Merten et al. (2001) found that the detachment rate decreased with increasing sediment load. However, their experimental results did not entirely support the concept of Foster and Meyer (1972, 1975). Lei et al. (2006) observed in laboratory experiments in an eroding rill using rare earth element tracers that for certain combinations of slope and discharge, sediment load affected the detachment rate and for other combinations it did not. Govers et al. (2007) explain these ambiguous results in the difficulty of studying the exclusive effect of sediment load on detachment in experiments. This is because of a feedback between the sediment flux and water flux arising from the transfer of kinetic energy from the stream to the sediments (Kleidon et al., 2013), which affects the capacity of the flow to detach and transport sediments.

Hairsine and Rose (1992b, a) propose that detachment and deposition occur simultaneously. They suggest that after the mobilization of soil particles from the flow bed, some are deposited and form a deposition layer, from which particles may be remobilized. The actual sediment load results from the interaction of three processes, namely (i) the entrainment of particles from the flow bed, (ii) the re-entrainment of particles from the deposition layer and (iii) the deposition of particles. The first two processes are regarded as being separable due to the different cohesion between the respective materials. Hairsine and Rose (1992b, a) suggested a coupled system of equations to describe these processes based on stream power. The key idea is to balance the ki-

HESSD
12, 3527–3592, 2015

netic energy of the flow and account for feedbacks due to kinetic energy transfer to the sediment. Although this equation system is not based on an empirical transport capacity, it is structurally identical to the model concept of Foster and Meyer (1972, 1975) (Yu, 2003; Merten et al., 2001; Govers et al., 2007). A major critique of the approach of Hairsine and Rose (1992b, a) is that sediment detachment and transport by overland flow are not necessarily controlled by the same hydraulic variables (Govers et al., 2007; Govers and Rauws, 1986).

We conclude that to date there is no clear experimental evidence that supports rejection of one or the other of the concepts outlined above describing the interaction of sediment transport and detachment. Some experiments support the concept of Meyer and Wischmeier (1969). Other experiments provide evidence that sediment load may affect detachment, while a first-order coupling seems questionable (Govers et al., 2007). A clear drawback of the concept of Foster and Meyer (1972, 1975) is that the detachment rate is largely dependent on the selected formulation of transport capacity. Such an interdependence reduces identifiability of the related parameters due to parameter interactions as shown by Bardossy (2007). To avoid this source of equifinality, we adopt the concept of Meyer and Wischmeier (1969) and treat detachment and sediment transport as separable and independent processes. Sediment delivery to the stream is thus limited either by the detachment rate or by the transport capacity of overland flow.

With respect to deposition of particles, both concepts of Foster and Meyer (1972, 1975) as well as of Hairsine and Rose (1992a, b) result in similar expressions, as shown by Beuselinck et al. (1999, 2002).

2.1.2 Detachment of soil particles

Detachment of soil particles and aggregates is triggered by the attacking forces of raindrop impact (splash erosion) and overland flow. On arable land splash erosion occurs primarily on inter-rill areas (Kinnell, 2005; Salles et al., 2000) while rill detachment is mainly caused by attacking fluid forces due to concentrated overland flow in micro-relief channels (Knapen et al., 2007). However, the spatial separation of rill and inter-rill ar-

HESSD
12, 3527–3592, 2015

eas is often not clearly defined, varies in time (Giménez and Govers, 2001; Lei et al., 1998; Nearing et al., 1997) and is not observable at larger scales. Models for catchment scale erosion and sediment yields thus often treat detachment by rainfall and overland flow in an effective lumped manner (Smith et al., 1995; Wicks and Bathurst, 1996; Heatwole et al., 1998; De Roo et al., 1998; Schmidt et al., 1999; Johnson et al., 2000), by merging the underlying attacking forces.

In CATFLOW-SED we implemented a semi-empirical approach (Eq. 4) that relates the potential detachment rate e_{pot} ($kg\,m^{-2}\,s^{-1}$) bi-linearly to the attacking forces of rainfall, characterised as rainfall momentum flux m_r ($N\,m^{-2}$), and overland flow, characterised as shear stress τ ($N\,m^{-2}$) (Scherer et al., 2012). The resisting forces acting against detachment are characterised by two empirical parameters: the erosion resistance f_{crit} ($N\,m^{-2}$) as well as the erodibility parameter p_1 (–), scaling the growth of the detachment rate in case the attacking forces exceed the threshold f_{crit}. The parameter P_2 (–) weighs the momentum flux of rainfall against shear stress from overland flow. The empirical parameters were determined for conventionally tilled loess soils using data from rainfall simulation experiments performed in the laboratory (Schmidt, 1996) and at erosion plots in the field (comp. Sect. 3.2.3 and Scherer et al., 2012):

$$e_{pot} = p_1 \cdot (\tau + P_2 \cdot m_r - f_{crit}) \quad \text{if } e_{pot} < 0,\ e_{pot} = 0. \tag{4}$$

We assume equal mobility of all particle sizes during the detachment phase, which implies that all particle size fractions and aggregates are mobilized according to their share in the top soil layer. This assumption is supported by grain size analyses of eroded loess material gained in rainfall experiments carried out in the Weiherbach catchment (comp. Sect. 3.2).

2.1.3 Transport of soil particles in overland flow and stream flow

Although the hydraulic conditions for stream flow and overland flow are different, stream flow equations are often implemented in soil erosion models due to the lack of widely tested approaches for overland flow. The most commonly used stream flow based approaches in erosion models are the bed load equation of Yalin (1972) and the total load equations of Yang (1973) and Engelund and Hansen (1967). Several studies tested the applicability of stream flow based equations for overland flow conditions using experimental data of transport rates derived in the lab (Alonso et al., 1981; Govers, 1992; Ferro, 1998; Nord and Esteves, 2007; Ali et al., 2013; Hessel and Jetten, 2007). Due to the particular experimental conditions, different equations performed equally well and none of them turned out to be generally superior. Julien and Simons (1985) theoretically evaluated the relationship between sediment transport rates and the dominant controls such as hillslope gradient, runoff rate for laminar and turbulent overland flow and compared the results with 14 stream flow equations. The approach of Engelund and Hansen (1967) was the only one that covered the whole range of overland flow conditions. Prosser and Rustomji (2000) performed a similar analysis using transport approaches for overland flow and stream flow. They conclude that sediment transport in overland flow and stream flow is controlled by the same processes and parameters and that stream flow equations are in principle – after proper calibration and validation - applicable for overland flow conditions.

Most of the transport approaches developed for overland flow conditions employ simple regressions between observed transport rates and hydraulic predictors for different sediment mixtures (Huang, 1995; Nearing et al., 1997; Ferro, 1998; Jayawardena and Bhuiyan, 1999; Tayfur, 2002; Zhang et al., 2009a; Everaert, 1991). More complex approaches were developed for example by Govers (1992), Guy et al. (2009a, b), Abrahams et al. (2001), Ali et al. (2013) or Li et al. (2011). All these approaches show a good correlation between observed and predicted transport rates for the experimental conditions under which they were developed. However, up to now only a few studies tested the extrapolation of the approaches to other conditions (Ali et al., 2013; Hessel and Jetten, 2007; Nord and Esteves, 2007; Nord et al., 2009). A comprehensive test for varying conditions and sediment properties under field conditions is still missing. In addition most of the experimental studies for overland flow used sandy, non-cohesive sediment material (Zhang et al., 2011; Ali et al., 2012) and the results are thus difficult to transfer onto fine cohesive soil material.

As there is to date no evidence that one of the above listed approaches is superior, we defined the following criteria to select an equation that meets our model requirements:

- The transport capacity equation should be sensitive to different grain size fractions and sediment densities, which is crucial for modelling particulate transport of nutrients and contaminants (Nadeu et al., 2011).

- Govers (1992) showed that bed load equations underestimate the transport capacity of fine particles smaller than the sand fraction. As Nord et al. (2009) have corroborated these findings, we consider bed load equations as inappropriate for loess soils.

- Various transport equations contain a threshold parameter for the incipient movement of grains and aggregates. However, several studies revealed that this threshold can be neglected for small grain sizes (Hessel and Jetten, 2007) and that all grain size fractions are simultaneously mobilized even under shallow flow conditions (Everaert, 1991; Li and Abrahams, 1999). For loess soils an equation without such a threshold for incipient motion should thus be preferred.

- An increased surface roughness significantly reduces the transport capacity of overland flow (Govers and Rauws, 1986; Abrahams et al., 2001). Following Govers (1992) we prefer equations based on hydraulic variables with a clear dependence on surface roughness.

Based on these criteria we selected the approach of Engelund and Hansen (1967) as most appropriate for our purpose (Eq. 5). Since Eq. (5) was developed for stream flow conditions, a calibration of the empirical parameters might be necessary (Prosser and Rustomji, 2000).

HESSD
12, 3527–3592, 2015

$$\phi = \frac{2}{5} \cdot \frac{\theta_i^{\frac{5}{2}}}{\lambda} \quad \text{with } \phi = \frac{T_\mathrm{c}}{\rho_\mathrm{p} \cdot \sqrt{g' \cdot d_\mathrm{m}^3}}, \ \theta_i = \frac{v_*^2}{g' \cdot d_\mathrm{m}}, \ \lambda = \frac{8 \cdot \tau}{\rho \cdot v^2}$$

$$\text{and } g' = \left(\frac{\rho_\mathrm{p}}{\rho_\mathrm{w}} - 1\right) \cdot g, \ v_* = \sqrt{\frac{\tau}{\rho_\mathrm{w}}} \tag{5}$$

where ϕ is dimensionless transport intensity, θ_i dimensionless stream intensity, λ dimensionless resistance coefficient, d_m mean particle diameter in m, g' modified acceleration of gravity in $\mathrm{m\,s^{-2}}$, g acceleration of gravity in $\mathrm{m\,s^{-2}}$, ρ_p density of particles $\mathrm{kg\,m^{-3}}$, ρ_w density of water $\mathrm{kg\,m^{-3}}$ and v_* friction velocity in $\mathrm{m\,s^{-1}}$.

Due to the narrow range of particle sizes of loess soils and the fact that cohesive loess material is transported in aggregated form (Beuselinck et al., 2000), we assumed equal mobility of all particle size classes during transport along the hillslope. This assumption is further supported by observations of Fuchs and Schwarz (2007) who measured no significant enrichment of clay and fine silt fractions in eroded soil material in a cultivated loess region in Southwest Germany. The apportionment of transport capacity on the various grain size fractions in a hillslope section is based on the frequency distribution of the grain size fractions within the transported sediment mixture and within the detached amount of surface soil material.

2.1.4 Deposition of soil particles

As particle deposition is controlled by the sinking velocity of suspended soil particles, it is a highly size selective process (Beuselinck et al., 2002, 1999, 2000; Nadeu et al., 2011). Generally, the process descriptions for deposition are based on two assumptions: (i) complete mixture of particles in overland flow and (ii) independence of the sinking velocity from overland flow conditions. The first assumption is justified during rainfall driven conditions, because the induced turbulence will enhance vertical mixing.

HESSD
12, 3527–3592, 2015

Beuselinck et al. (1999) corroborated the validity of the second assumption by comparing observed particle size fractions from sediment transport experiments in a laboratory flume over an area of net deposition. They found that the observed and predicted deposition rates matched well when using approaches to quantify the sinking velocities which were derived for fluids at rest.

Equation (6) determines the sinking velocity v_s ($\mathrm{m\,s^{-1}}$) of a spherical particle in a fluid at rest based on the balance of the drag force, gravity and buoyancy.

$$v_s = 2 \cdot \sqrt{\frac{g' \cdot d_m}{3 \cdot C_w}} \tag{6}$$

where v_s is sinking velocity in $\mathrm{m\,s^{-2}}$ and C_w dimensionless drag coefficient. The drag coefficient C_w depends on the Reynolds number Re related to the particle stream (Eq. 7).

$$Re = \frac{v_s \cdot d_m}{\nu} \tag{7}$$

where ν is kinematic viscosity $\mathrm{m^2\,s^{-1}}$ of the fluid.

For higher Reynolds numbers ($Re > 0.1$) inertia forces cannot be neglected. For these conditions a range of experimentally determined approaches are available, as for instance the relationship of Kazanskij (1972), which is valid for $Re \leq 4.3 \times 10^3$ and thus including the Stokes' range (Eq. 8).

$$C_w = \frac{24}{Re} + \frac{5.6}{\sqrt{Re}} + 0.25 \tag{8}$$

The sinking velocity of particles increases with increasing sediment concentration (Beuselinck et al., 1999; Hessel, 2006). Equation (9) presents the adaptation of the sinking velocity for particle swarms.

$$v_{s,ps} = v_s \cdot (1 - c_v)^b \tag{9}$$

HESSD

12, 3527–3592, 2015

Predicting land use and soil controls on erosion and sediment redistribution

U. Scherer and E. Zehe

where $v_{s,ps}$ is the sinking velocity of particles in a particle swarm and b the dimensionless empirical parameter. Wan and Wang (1994) suggest a constant value of 5 for the empirical parameter b.

The deposition rate in a model discretization element depends on the question of whether a particle reaches the flow bed within a certain discretization element and time step or not. The vertical travel distance of a particle in a certain time step can be calculated based on the relationship of the sinking velocity and the lateral flow velocity (Eq. 10) and travel distance of the particle Δx (m).

$$\Delta y = \frac{v_s}{v_p} \cdot \Delta x \tag{10}$$

The proportion of particles deposited within the time step Δt is equal to the ratio of Δy to the flow depth h (Eq. 11).

$$C_{dep} = \frac{\Delta y}{h} = \frac{v_s}{q} \cdot \Delta x \tag{11}$$

where C_{dep} is dimensionless coefficient of deposition and q flow rate per unit width $m^2\,s^{-1}$.

Foster (1982) found in laboratory experiments that the coefficient of deposition diminished under rainfall driven conditions due to increased turbulence. Based on the results of the experiments Foster (1982) suggested decreasing of C_{dep} by a factor of 0.5.

2.2 From CATFLOW to CATLFOW-SED

2.2.1 Model structure and water balance components

CATFLOW is a continuous, spatially distributed model for water dynamics at the hillslope and small catchment scale (Zehe et al., 2001; Plate and Zehe, 2008; Maurer,

HESSD
12, 3527–3592, 2015

1997). The model represents a hillslope catena along the steepest descent line as a two-dimensional cross-section that is discretized using curvilinear orthogonal coordinates. The size and number of model elements in the cross-section of individual hillslopes can be chosen as required. Each surface model element extends over the width of the hillslope, which can vary from the top to the foot of the slope. At the catchment scale, the hillslopes are connected to a drainage network of permanent and temporal streams. Water dynamics is described by the Richards equation in the mixed form that is numerically solved by an implicit mass conservative Picard iteration. The simulation time step is dynamically adjusted to achieve an optimal change of the simulated soil moisture per time step, which assures fast convergence of the Picard iteration.

Accordingly, the model allows simulation of subsurface flow under saturated and unsaturated conditions. The shape of the retention curve is parameterized using the van-Genuchten model (Mualem, 1976; van Genuchten, 1980). Macropore flow is represented by a simplified, effective approach that increases local hydraulic conductivity (Eq. 12). To account for high unsaturated conductivities at high water saturation values, we used a threshold value RS_0 for the relative saturation RS, which is motivated by the experimental findings of Zehe and Flühler (2001). If RS at a macroporous grid point at the soil surface exceeds this threshold, the bulk hydraulic conductivity at this point is assumed to increase linearly.

$$
\begin{aligned}
&k_{s,\,tot} = k_s + k_s \cdot f_m \left(\frac{RS - RS_0}{1 - RS_0} \right) \quad \text{if } RS \geq RS_0 \\
&k_{s,\,tot} = k_s \qquad \text{otherwise} \\
&RS = \frac{\theta - \theta_r}{\theta_s - \theta_r} \qquad (12)
\end{aligned}
$$

where RS is dimensionless relative saturation, RS_0 threshold value for relative saturation indicating the beginning of preferential flow (dimensionless), k_s saturated hydraulic conductivity of the soil matrix in $m\,s^{-1}$, $k_{s,\,tot}$ bulk hydraulic conductivity of the soil matrix and the macropore system in $m\,s^{-1}$, f_m dimensionless macroporosity factor, θ soil

HESSD
12, 3527–3592, 2015

Predicting land use and soil controls on erosion and sediment redistribution

U. Scherer and E. Zehe

moisture in $m^3 m^{-3}$, θ_s and θ_r saturated and residual soil moisture, respectively in $m^3 m^{-3}$.

Evaporation and transpiration are simulated using an advanced approach based on the Penman–Monteith equation, which accounts for annual cycles of plant morphological and physiological parameters, albedo as a function of soil moisture and the impact of local topography on wind speed and radiation.

The model simulates overland flow as sheet flow using the diffusion wave equation, which is a simplification of the Saint–Venant equations for shallow water flow. The diffusion wave equation is composed of the continuity equation for mass conservation (Eq. 13) and the dynamic core equation (Eq. 14). In contrast to the Saint–Venant equations, the acceleration terms are neglected in Eq. (14) in the diffusion wave approach.

$$\frac{\partial h}{\partial t} = -\frac{1}{b} \cdot \frac{\partial (A \cdot v)}{\partial x} + \frac{q_{lat}}{b} \tag{13}$$

$$g \cdot \frac{\partial h}{\partial x} - g \cdot (S_0 - S_e) = 0 \tag{14}$$

where b is flow width in m, A flow cross section in m^2, v flow velocity in $m s^{-1}$, q_{lat} lateral inflow in $m^2 s^{-1}$, S_0 topographical gradient of the hillslope and S_e gradient of the water level.

Flow velocity is quantified based on the Manning–Strickler-formula. Flow in the drainage network is also simulated based on the kinematic wave approach.

2.2.2 Coupling of water and sediment budgets

The process representations for erosion and sediment redistribution derived in Sect. 2.1 were implemented in a separate module in CATFLOW-SED. The hydraulic variables flow depth h, flow velocity v and gradient of the water level S_e, which are calculated for each discretization element and time step, constitute the interface for the direct coupling of overland flow and erosion. Figure 1 presents the discretisation scheme for the numerical simulation of overland flow based on the diffusion wave.

As shown in Fig. 1 the hydraulic variables vary along the flow path and thus within the discretization elements. Therefore the hydraulic input variables used for simulating the erosion sub-processes have to be carefully selected. The potential detachment rate per area e_{pot} is calculated based on Eq. (4). The *total* detachment rate per unit width $q_{s,\,pot}$ ($kg\,m^{-1}\,s^{-1}$) for each discretization element is thus given by integrating the area-specific potential detachment rate e_{pot} along x (into downslope direction, Eq. 15):

$$q_{s,\,pot} = \int_{x_{i-1}}^{x_i} e_{pot} \cdot dx \tag{15}$$

Due to the threshold character of particle detachment, detachment starts at the downslope location where the attacking forces of rainfall and shear stress exceed the erosion resistance. This point needs to be determined by integration and a coarse spatial discretization implies a spatial uncertainty. To overcome this problem, each discretization element above a critical length is further discretized into sub-elements during computation. The average flow depths are interpolated for each sub-element and the potential detachment rate e_{pot} is quantified. The total potential detachment rate $q_{s,\,pot}$ of the given discretization element is obtained by numerical integration of detachment rates of the sub-elements along the extent of the model element. A sensitivity analysis revealed that a good approximation of Eq. (15) is reached for a sub-element length of 1 m. With this the spatial discretization for overland flow simulation can remain of the order of 10–20 m, which considerably reduces computation time due to the explicit time stepping.

As the transport capacity integrates the capacity of overland flow to transport sediments over the flow length per unit width, we used hydraulic variables calculated at the end of each discretization element for its calculation. The deposition coefficient C_{dep} (Eq. 11) was determined using the average flow velocity and flow depth within each element as relevant input variables.

HESSD
12, 3527–3592, 2015

3 Study area, experimental data base and model setup

3.1 The Weiherbach catchment

The Weiherbach catchment is located in a hilly loess region in Southwest Germany (Fig. 2). The climate is semi humid with an annual precipitation of 800 mm yr^{-1}, annual runoff of 150 mm yr^{-1}, and annual potential evapo-transpiration of 775 mm yr^{-1}. The bedrock is composed of lower and middle Keuper (Gipskeuper and shilf sandstone) which is almost completely covered by a loess layer that reaches to a massive 15 m (Fig. 3). The loess in the Weiherbach catchment is highly calcareous (25–30 % lime by weight), the percentage of coarse silt ranges between 50–55 % and the porosity between 0.45 and 0.50.

More than 90 % of the catchment area is arable land or pasture, 7 % is forested and 2.5 % is paved (farm yards and rural roads). The predominant crop rotation types are the short maize – winter wheat rotation and the multiple sugar beet – winter wheat – spring barley – maize – (sun flower) – winter wheat – maize rotation. The tillage practice is mainly conventional with a ploughing depth of 30–35 cm in early spring or early autumn depending on the crop type. In the Kraichgau region, severe runoff and erosion events are typically caused by thunder storms in late spring and summer.

Due to the absence of lateral subsurface strata and the huge loess layers, Hortonian overland flow dominates event runoff generation. Because the apparent macropores elevate infiltrability of soils, rainfall runoff events are rare. Event runoff coefficients range from 12 % during extreme thunder storms down to only 2 %. Base flow is almost constant throughout the year.

HESSD
12, 3527–3592, 2015

3.2 The Weiherbach data set

3.2.1 Hydro-meteorological data

Figure 2 presents a map of the monitoring network in the northern part of the Weiherbach catchment, which has been established since the 1990s (Zehe et al., 2001; Plate and Zehe, 2008) during an interdisciplinary research project on water, sediment and material flow in intensively cultivated areas. Discharge and rainfall data were measured at gauge Menzingen (3.5 km^2) and several rain gauges at a resolution of 6 min. Standard meteorological variables were recorded at the central meteorological station in an hourly time step. Soil moisture was measured at 61 locations in intervals of 1–2 weeks using two-rod TDR equipment that integrates over 15, 30, 45 and 60 cm of soil depth, respectively.

3.2.2 Soil hydraulic properties, macropores and land use

A soil map was compiled using data from field mapping and additional soil texture information. The soil type pattern turned out to be highly organized: most of the hillslopes exhibit a typical loess catena with calcaric regosol soils at the hill top and mid slope and Colluvisol soils located at the hill foot due to erosion caused by intensive cultivation in the catchment over a long period (Fig. 3). The soil hydraulic properties after van Genuchten–Mualem (van Genuchten, 1980; Mualem, 1976) were measured in the laboratory using undisturbed soil samples taken along transects at several hillslopes (Table 1) (Plate and Zehe, 2008).

The macropore system consists of anecic earthworm burrows (*Lumbricus terrestris* and *Aporectodea longa*). The macropore system was mapped at 15 sites in the Weiherbach catchment, at which horizontal soil profiles were prepared. For each profile macropores that were connected to the soil surface were counted and their depth and diameter were measured using a vernier caliper and a wire. In addition sprinkling experiments with brilliant blue were carried out to analyze preferential flow patterns. The

HESSD
12, 3527–3592, 2015

spatial pattern of macroporosity was closely related to the soil catena. The macroporosity tends to be lower in the dryer calcaric regosols located at the hilltop and mid slope, than in the colluvisols at the hill foot, which are typically moister due to higher contents of organic matter and clay. This spatial organization pattern along the hillslopes may be explained by the habitat preferences of *Lumbricus terrestris* which is the dominating anecic earthworm species in the Weiherbach (Zehe and Flühler, 2001; van Schaik et al., 2014). In addition the number of earthworm borrows connected to the surface varied throughout the year, since their connectivity is partly destroyed by ploughing. After tillage, the pore system is rebuilt by the earthworms (Zehe and Blöschl, 2004).

The pattern of main crops and catch crops was mapped in several campaigns. Table 2 presents the percentage of land use for the main crop periods of 1994 and 1995 (April–September), Fig. 4 displays the land use pattern in 1994. The crop phenological and physiological parameters of the dominant crop types such as plant height, root depth, percentage of soil cover, surface roughness, leaf area index and stomatal resistance were determined during the growth period.

3.2.3 Sediment loads in the river, short and long term erosion experiments

Sediment concentrations in the Weiherbach at gauge Menzingen (Fig. 2) were recorded during runoff events by using automatic water samplers (Hahn and Beudert, 1997). Sediment concentration was analyzed in the lab and the sediment load for discrete events was calculated from sediment concentration and discharge data.

During the monitoring period three strong erosion events have been observed (Table 3). The largest event occurred on 24 June in 1994 with a cumulative rainfall of 83 mm in 3 h and a peak discharge of 7.92 $m^3\,s^{-1}$ at gauge Menzingen. During this event part of the storm runoff bypassed the weir and the volume had to be reconstructed from the flooded bank area using hydraulic calculations. The second largest event occurred on 13 August 1995. Although the cumulative rainfall amount of 73.6 mm and antecedent wetness were similarly high as for the event in 1994, the peak discharge reached only 50 % of the peak discharge of the largest event. Apparently, the

HESSD
12, 3527–3592, 2015

infiltration capacity of the soils was much higher than in June 1994. In August 1994, a smaller event was observed with a flood volume comprising 10 % of the volume of the largest event in June 1994. The balanced sediment loads at gauge Menzingen reveal a strongly non-linear dependence on discharge volume with a maximum sediment load of nearly 2000 t for the event in June 1994 (Table 3).

To quantify the erodibility and erosion resistance of the loess soils in the Weiherbach catchment, 58 rainfall simulation experiments have been carried out within the years 1993–1995 (Gerlinger, 1997; Gerlinger and Scherer, 1998). A transportable rainfall simulator was used that consists of modular elements. For 56 experiments an area of 2 m in width and 12 m in length was irrigated while two experiments were carried out on larger plots. The total range of rainfall intensity varied between 34 and 62 mm h^{-1}. The experiments were conducted in different seasons (spring and late summer) to examine varying soil conditions e.g. initial soil moisture. Most of the experiments were performed on bare soil after seed bed preparation. Additionally, 11 experiments were carried out to investigate the highly erodible row crops maize and sugar beet during the growing period. At the end of the irrigated area a channel was installed to collect the runoff. Water samples were taken manually every minute, starting with the onset of surface runoff generation, to measure the runoff rate. Sediment concentrations in the runoff samples were measured in every third sample in the lab. At each experimental site antecedent soil moisture was measured gravimetrically in soil samples taken at a depth of 5–10 cm. Particle size distribution (clay, fine, middle and coarse silt, fine, middle and coarse sand) and organic content of the top soil were measured in the lab. The roughness coefficients of the plots (Mannings *n*) were estimated by fitting the falling limb of the observed hydrograph after irrigation was terminated (Engman, 1986; Govers et al., 2000). Further details on the experimental setup are given by Gerlinger (1997), Seibert et al. (2011) and Scherer et al. (2012).

In addition to the rainfall simulation experiments a long-term soil erosion plot of 69 m in length and 4 m in width was set up on a hillslope in the Weiherbach catchment with a gradient of 13 % (Fig. 2). At the lower end, a tank was installed to collect runoff and sediment from the plot. During the extreme soil erosion event on 27 June 1994 a sediment load of 1.17 t was collected in the tank. The runoff volume could not be measured, since the tank was flooded. We thus assume that the total soil loss of the plot was above the measured quantity. At 27 June 1994 sugar beet was cultivated on the plot in the direction of slope with a soil cover of 90 %.

3.2.4 Regionalization of erosion resistances based on rainfall experiments

Based on the rainfall experiments the detachment rates and erosion resistance f_{crit} (Eq. 4) were determined for each irrigation site. In order to regionalize these plot scale results to the catchment, the erosion resistance was related to candidate predictors such as clay content, organic content, antecedent soil moisture, surface roughness, crop type and percentage of vegetation cover of the erosion plots (Scherer et al., 2012). This analysis revealed cultivation and land use as the first order control of the erosion resistance, because the soil texture is rather homogeneous in the Weiherbach. Experiments conducted at sites covered by maize and sugar beet revealed systematically small erosion resistances without significant correlations to soil properties. These crops are strongly susceptible to detachment because runoff is channelled along the intermediate areas of plant rows. Since the effect of the concentrated flow regime surpasses other possible influencing factors, we chose a constant average erosion resistance of $0.73\,\mathrm{N\,m^{-2}}$ for maize and sugar beet.

For bare soils we found a strong correlation between the erosion resistance, surface roughness according to Manning–Strickler n ($\mathrm{m\,s^{-1/3}}$) and clay content CC (%) which explained 70 % ($R^2 = 0.70$, significant at the 0.1 % level) of the observed variance within a bilinear regression.

$$f_{\mathrm{crit}} = 0.061 + 17.991 \cdot n + 0.014 \cdot \mathrm{CC} \tag{16}$$

Further details on the monitoring network installed in the Weiherbach catchment are given by Zehe et al. (2001) and Plate and Zehe (2008).

HESSD
12, 3527–3592, 2015

3.3 Model verification and scenario setup

3.3.1 Hierarchical verification procedure

The components of the erosion module of CATFLOW-SED are verified along the hierarchy of scales which is characteristic for the three governing processes. The approach for characterizing particle detachment (Sect. 2.1.2) is verified based on the rainfall simulation experiments, as sediment transport capacity is not the limiting factor at this scale. On the hillslope sediment transport capacity is regarded as the limiting factor and sediment deposition gains importance when moving to the entire catchment (Sects. 2.1.3 and 2.1.4). To test our choices to characterize transport capacity we thus chose the sediment loads eroded from the long term plot during the heavy storm event in June 1994. The simulated integral response of all erosion processes at the catchment scale is tested against sediment loads monitored at gauge Menzingen for the three storms observed during the project period (Sect. 3.2.).

A highly accurate simulation of surface runoff on the event scale is pivotal for verification of the proposed modelling approaches for erosion, as the errors in simulated runoff directly propagate to the simulated sediment loads (Sect. 2.2.1). The model was thus in a first step calibrated to reproduce runoff. Following the procedure of Zehe and Blöschl (2004) the average macroporosity factor f_m (Eq. 12) of the hillslopes was used as a calibration parameter, since the number of macropores connected to the surface varies throughout the year and is very difficult to measure (Sect. 3.2) (van Schaik et al., 2014). As goodness of fit measures we used the balance error BIAS, the root mean square error RMSE and the Nash Sutcliffe efficiency E (Nash and Sutcliffe, 1970).

3.3.2 Plot scale simulation of rainfall experiments

For validation of the detachment approach, 39 rainfall simulation experiments were modelled with CATFLOW-SED as these experiments cover the entire range of possible hydrological conditions: 19 experiments were performed under very dry conditions in late summer (between 23 August and 3 September) and 20 experiments under wetter conditions in spring (between 29 March and 22 April). The rainfall simulation plots were discretized in a cross- section scheme of 21 lateral and 29 vertical model elements covering a depth of 1 m. For the model setup of each experiment, measured values of initial soil moisture of top soil, soil hydraulic parameters, surface roughness, percentage of soil cover, soil texture as well as intensity and duration of irrigation were included. Initial soil moisture in deeper layers of the soil profile was not measured and therefore interpolated using the data set gained from TDR monitoring (Sect. 3.2). Each experiment was modelled by a stepwise increase of the macroporosity factor until the simulated surface runoff volume matched the observed runoff volume. The calibrated macroporosity factors were then correlated to the soil properties clay content, organic matter content and initial soil moisture since a positive correlation between these parameters and the density of macropores was observed during mapping campaigns in the catchment (Sect. 3.2). The objective of this task was to find a simple approach to regionalize the macroporosity factor f_m. Finally each rainfall simulation experiment was modelled using the best specific parameter sets for the macroporosity factor f_m and the erosion resistance f_{crit}. In addition, the sensitivity of the parameters was analyzed (see Sect. 3.3.5).

3.3.3 Hillslope scale: long term soil erosion plot

Erosion on the long term soil erosion plot was simulated for the heaviest observed storm event in the Weiherbach catchment on 27 June 1994. The soil erosion plot was discretized using the same vertical discretization scheme as for the rainfall simulation plots (Sect. 3.3.2). The length of the model elements was set to 3.3 m each. Figure 5 presents a cross-section of the topography (Fig. 5, top) and the discretization in lateral model elements along the hillslope (Fig. 5, bottom). Soil texture of the calcaric regosol at the hill top is classified as loamy silt and as very loamy silt for the colluvisol at the hill foot (Table 4). In the model setup a transition zone between both soil types/textures was assumed (Fig. 5, top). During the vegetation period in spring 1994 rainfall simulation experiments were carried out on sugar beet in the neighborhood of the long term soil erosion plot (Fig. 2). For the model setup we used the macroporosity factor f_m of one of these experiments, which was carried out a few days before the storm event (17 June 1994, $f_m = 2.6$). It was assumed that the macroporosity factor increases along the hillslope according to the findings of Zehe et al. (1999). The erosion resistance was set to $f_{crit} = 0.73$ for sugar beet. Surface roughness (Mannings n) was measured for sugar beet as $0.036\,\mathrm{s\,m^{-1/3}}$. Initial soil moisture was interpolated from the TDR monitoring data set. For the simulation of the storm event, the rainfall data measured at the meteorological station were used which is near the soil erosion plot (Fig. 2).

3.3.4 Catchment scale: Weiherbach catchment

At the catchment scale we simulated the three largest storm events. For the catchment simulations we used the discretization scheme and the organisation pattern of soil types and macroporosity suggested in former hydrological modelling studies with CATFLOW (Zehe and Blöschl, 2004; Plate and Zehe, 2008). The catchment was subdivided into 169 hillslopes, which are connected to a temporary drainage network (Fig. 6a). Each slope was represented by a cross-section along the line of the slope. Figure 6b presents the top view of the discretisation elements of each hillslope. The typical loess catenas in the Weiherbach catchment (Sect. 3.2) were represented by a sequence of 80 % calcaric regosol (hill top and mid slope) and 20 % colluvisol (hill foot) with regard to the length of the hillslopes. As presented in Sect. 3.2, this high degree of spatial organisation of soil types induces a structured organisation of biogenic macroporosity. The hydraulic conductivity of macroporous colluvisols at the hill foot is about 1.5–2.5 times higher than the hydraulic conductivity of calcaric regosols at the hill top where less macropores were found (Schäfer, 1999; Zehe, 1999).

To account for this structured variability in the model parameterization, we used scaled values of the macroporosity factor f_m (Eq. 12) at each hillslope: at the upper 70 % of the hillslope a macroporosity factor of $f_m = 0.8$ was used, while at the mid slope ranging from 70 to 80 % and the hill foot ranging from 85 to 100 % a factor of $f_m = 1.0$ and $f_m = 1.3$, respectively, was used to represent the observed relationship of hydraulic conductivities and macropore volumes. The depth of the macroporous layer was assumed to be constant throughout the whole catchment and was set to 0.4 m. On the basis of the given soil hydraulic parameters (Table 1) and the spatial variability of macroporosity, the only remaining free parameter is the average macroporosity factor f_m which has to be calibrated to adapt the runoff simulation for the three specific runoff events in the Weiherbach catchment.

Soil texture was determined from the soil map for each surface model element. In the Weiherbach catchment, five soil textures can be differentiated. Each type is parameterized by the percentage of 8 grain size fractions (Table 4). The erosion resistance was regionalized to the catchment area according to the procedure presented in Sect. 3.2 (Scherer et al., 2012). The crop type and growth stage of vegetation for the point in time of the three storm events was determined for each surface model element from the mapped cropping pattern and time series of plant growth parameters.

The model was driven with observed time series of rainfall and climate variables. For initial soil moisture conditions, average values of the TDR monitoring data set measured shortly before each event were used, as specified in Zehe and Blöschl (2004).

3.3.5 Sensitivity analysis and land use scenarios

The macroporosity factor f_m and the erosion resistance f_{crit} are deemed to be the most sensitive model parameters of CATFLOW-SED. The sensitivity to the runoff and erosion response was tested by varying both parameters in the simulation of the plot scale experiments. The sample experiments are the same as for the verification step (Sect. 3.3.2). Each experiment was modelled using (i) the optimum macroporosity factors (Sects. 3.3.2 and 4.1.1) and predicted erosion resistances (Sect. 3.2.4, Eq. 16), (ii) the predicted macroporosity factors (Sects. 3.3.2 and 4.1.1) and optimum erosion resistances and (iii) predicted macroporosity factors and predicted erosion resistances.

HESSD
12, 3527–3592, 2015

In order to test the capability of the model to analyze land use scenarios, we varied the given land use pattern for the main crop period of 1994 (Table 2, Fig. 4a) and simulated the strongest observed storm event in the Weiherbach catchment on 27 June 1994. The land use pattern of 1994 was rearranged in a "best case" and a "worst case" scenario whereby the percentage of the land use categories was kept constant. To assess the spatial pattern of susceptibility for erosion as a function of topography, soil texture and macroporosity, the storm was first simulated for bare soils (Fig. 4b). Based on this analysis we re-arranged the land use pattern within the field borders. For the "best case" scenario the grass land was located on the highly erosive steep slopes in the east of the catchment, grain was placed on areas with a medium erosion risk and row crops such as corn, sugar beet and sun flower were arranged on fields with shallow slope. For the "worst case" scenario grassland and grain were placed on areas with a low susceptibility to erosion while crops with a high erosion risk were located on the steep slopes except for the very steep south-eastern slopes: these slopes are covered with pasture in the given land use pattern, which was retained since it is unlikely that the steep slopes would be cultivated to carry a crop. In addition, the forested and sealed areas were retained in both scenarios. Figure 7 presents the land use patterns for both scenarios.

4 Results

4.1 Verification of CATFLOW-SED at various scales

4.1.1 Rainfall simulation experiments

Figure 8 presents the range of macroporosity factors that was necessary to fit the runoff observed within the 39 experiments. The optimal f_m factors for experiments in late summer are on average higher (mean $f_m = 3.0$, median $f_m = 3.0$) than for the campaign in spring (mean $f_m = 2.2$, median $f_m = 1.9$). These differences can be explained

HESSD
12, 3527–3592, 2015

Predicting land use and soil controls on erosion and sediment redistribution

U. Scherer and E. Zehe

by tillage practice: the vertical worm burrows are cut by tillage in spring and rebuilt during the vegetation period. Thus by the end of the vegetation period in late summer, a seasonal maximum of macropores connected to the soil surface is reached (Beven and Germann, 1982; Zehe, 1999).

Figure 9 presents the observed and modelled hydrograph for a selected experiment. We simulated soil detachment using the best fit macroporosity factors and measured erosion resistances to reproduce the observed soil loss. Figure 10 presents the comparison of observed and modelled detachment volumes for the 39 experiments. The detached soil volume is slightly over-predicted with a BIAS of 3.4 kg (mean detached soil volume (observed): 65.8 ± 48.7 kg, mean detached soil volume (simulated): 69.3 ± 47.3 kg). The model efficiency E at 0.95 is very good. Overall, the agreement between observed and simulated detachment volume during the calibration phase is very good. The small deviations between observed and simulated detachment volumes are due to discrepancies between the shape of measured and modelled hydrographs and the assumption that the erosion resistances are constant during the rainfall simulation experiments.

In a last step the calibrated macroporosity factors were correlated with the clay content, initial soil moisture and the content of organic matter of the irrigation plots (Table 5). The highest regression coefficient for the entire sample was achieved for the linear regression of f_m to clay content with an R^2 of 0.46. The coefficient of determination increases when the summer and spring campaign samples are treated separately. For the spring period and the summer period the R^2 is 0.66 and 0.51, respectively. Note that the slope of the regression equations is 0.17 (Table 5) for both measuring campaigns. For organic matter content a regression coefficient of $R^2 = 0.31$ was reached for the spring sample, while the R^2 for both the summer sample and the sample containing all experiments was much lower (Table 5). However, the clay and organic matter contents of all 39 irrigation plots are positively correlated (R^2 of 0.3) so that consideration of organic matter content in addition to clay content in a multi-linear regression analysis did not show a positive effect on the coefficient of determination.

4.1.2 Heavy storm event at the long term soil erosion plot

Figure 5 (bottom) presents the area-specific erosion and deposition rates simulated for the largest storm event, on 27 June 1994. In the upper and middle region of the hillslope, the erosion rates are controlled by the topographic gradient, which is reflected in the high erosion rates in the mid slope. In the transition zone (Fig. 5, top) and at the flatter hill foot the infiltration capacity increases due to the elevated macroporosity, thereby decreasing overland flow sediment transport capacity and the surplus particles are deposited. In total, a runoff volume of $3.9\,m^3$ was calculated for the storm event, corresponding to a runoff coefficient of 18 % for the erosion plot. The simulated runoff volume cannot be verified, since the tank installed at the end of the erosion plot was flooded. The simulated soil loss is 1.3 t: in total, 1.5 t were eroded and 0.24 t were deposited at the hill foot. With respect to the error margin this corresponds very well with the observed sediment mass of 1.2 t. We thus conclude that the selected approach for simulating the transport capacity of overland flow is well suited for this loess soil landscape.

4.1.3 Erosion events at the catchment scale

At the catchment scale (Sect. 3.3.4) we simulated the three largest erosion events, the target variables being the river discharge and sediment loads at gauge Menzingen. Figure 11a presents the rainfall intensities as well as the observed and simulated hydrograph for the storm event on 27 June 1994. The best fit of the modelled hydrograph was achieved when using an average macroporosity factor $f_m = 2.1$. Overall, the shape of the main hydrograph was well represented by the model, with a model efficiency of 0.98. Differences between observed and modelled hydrographs are within the range of measurement uncertainty. The third largest event occurred 6 weeks after the largest event on 12 August 1994 (Table 3). The best fit of the corresponding hydrograph ($E = 0.98$) was achieved with the same average macroporosity factor $f_m = 2.1$ as for the largest event in June. This value is slightly larger as it is the mean of the best macroporosity factors that were obtained during simulation of the spring plot scale rainfall simulation experiments.

Figure 11b presents the modelled and predicted hydrographs of the second largest observed event that occurred on 13 August 1995. Although this rainfall event was very similar to the largest event in June 1994 as regards initial conditions, rainfall amount and intensity, the observed runoff volume was comparably small, with only two-thirds of the volume of the largest event. A reasonable fit for this event required a higher average macroporosity factor of $f_m = 3.35$. This increase can likely be explained by a higher surface density of worm burrows in August. Again this value corresponds well with the mean of the best macroporosity factors that were obtained during simulation of the summer plot scale rainfall simulation experiments (Sect. 4.1.1).

Based on these optimum macroporosity values, erosion and deposition were simulated for the three events, respectively. The predicted sediment loads agree well with the observed ones, the slight over-prediction is within the error margin of the observation (Table 6). Figure 12 displays the spatial pattern of the simulated cumulative erosion (a) and deposition rates (b) for the largest storm event on 27 June 1994. Areas covered with highly erodible crop types cultivated in rows such as corn, sugar beet and sunflower reveal high erosion rates, in particular when these crop types are located on the steep convex shaped slopes in the east of the catchment (Fig. 4). The average cumulative erosion rates for these crop types vary between 2.0–2.5 $\mathrm{kg\,m^{-2}}$ with the highest rates for sunflowers, since they were mainly located on the eastern hillslopes. The cumulative erosion rates for wheat were much lower with an average value of 0.8 $\mathrm{kg\,m^{-2}}$ due to the high soil cover ratio of about 80 % in late June. For forested or grass covered areas the erosion rates were low, as expected.

In total, 26 % of the detached soil material was deposited in the catchment. Retention areas are mainly located on plain areas along the temporary channel network and on hillslopes with a complex geometry (Figs. 12b and 4b). The total simulated deposition rate for the other two storm events was with 19 % (13 August 1995) and 12 % (12 August 1994) lower than for the event on 27 June 1994. An analysis of the spatial

HESSD
12, 3527–3592, 2015

variation of erosion showed that the main source areas were located on the steep convex shaped hillslopes in the east of the catchment. These convex shaped hillslopes have no distinct plain areas at the hill foot which is why the sedimentation rate was lower for these two smaller events. Beuselinck et al. (2000) monitored deposition rates in two small cultivated loess catchments in central and east Belgium. The catchment area, mean slope and land use of both catchments is comparable to the Weiherbach catchment. Beuselinck et al. (2000) report deposition rates of 25 and 40 %, respectively, for two thunderstorms in summer (16 mm 15 min^{-1} and 49 mm 30 min^{-1}). The simulated deposition rates for the Weiherbach catchment therefore seem plausible in comparison to the findings of Beuselinck et al. (2000).

4.2 Sensitivity and scenario analysis

4.2.1 Sensitivity analysis of the model parameters

To analyse the sensitivity of the model output due to the variation of the macroporosity factor f_m and the erosion resistance f_{crit}, we repeated the simulations of the rainfall experiments using different combinations of optimum and predicted values of both parameters (Table 7). The use of predicted values for the macroporosity factor decreased the model efficiency from $E = 0.97$ to $E = 0.66$ (Fig. 13a for runoff volumes). For predicted values of the erosion resistance parameter, the model efficiency of simulated detachment rates decreased from $E = 0.95$ to $E = 0.56$ (for specific macroporosity factors) and $E = 0.46$ (for predicted macroporosity factors), respectively (Table 7 and Fig. 13b). Despite the spread of data points, the cumulative runoff volumes and detachment rates were neither systematically over- nor under-estimated, which is shown by the low systematic errors of −0.01 m^3 and +4.87 kg (Fig. 13).

4.2.2 Land use scenarios

The "best case" and the "worst case" scenarios of the given land use percentage for 1994 (Sect. 3.2.4, Fig. 7) were modelled for the storm event on 27 June 1994 and the results were compared to the observed sediment yield at gauge Menzingen. For the "best case" scenario the sediment yield was reduced to 1147 t (40 % reduction) while it was increased to 2427 t (30 % increase) for the "worst case" scenario. The proportion of deposition for the "worst case" scenario was 25 % which is in the same range as for the given land use pattern. For the "best case" scenario it was increased to 32 %. This is mainly because the convex shaped slopes in the east of the catchment were covered with pasture in this scenario while the erodible arable land was placed on convex-concave shaped hillslopes with a distinct deposition area at the hill foot. Both scenarios show the importance of the land use pattern in the catchment. The sediment yield at the catchment outlet can be reduced by 40 % for an optimal arrangement of the land use pattern. However, both scenarios were idealized, since agricultural and economic aspects such as crop rotation were not considered.

5 Discussion and conclusions

The objective of this study was to develop, parameterize and verify a process-based soil erosion model for the catchment scale, which balances necessary complexity with greatest possible simplicity. We used the hydrologic model CATFLOW as a platform and further developed it to CATFLOW-SED by integrating approaches to simulate soil erosion and deposition in a loess landscape. The model was validated on a hierarchy of scales at which either particle detachment or sediment transport capacity or particle deposition are the limiting factors. For validation of the soil detachment approach, rainfall simulation experiments on the plot scale were modelled (Sect. 4.1.1). Sediment transport was verified on the hillslope scale by using data from a long-term soil erosion experiment (Sect. 4.1.2). Finally, erosion and deposition were simulated at the catch-

HESSD
12, 3527–3592, 2015

ment scale and the integrated sediment flux was compared against observed sediment loads of three heavy storm events at the catchment outlet (Sect. 4.1.3). For the verification of the implemented erosion approaches, the runoff simulation of CATFLOW-SED was calibrated by adapting the macroporosity factor f_m (Sect. 3.3.1). CATFLOW-SED predicted the sediment loads at all scales very well, with good agreement between simulated and observed runoff. The differences between simulated and observed sediment loads were within the error margin of the measurements so that no further calibration of the erosion approaches was necessary.

The governing process representations depend further on the spatial and temporal variability of the model parameters. Besides directly measured input data such as precipitation, initial soil moisture, soil hydraulic properties, soil texture, soil cover, etc., the most important model parameters are the erosion resistance f_{crit} and the macroporosity factor f_m. We analyzed the sensitivity of both parameters on the plot scale by using optimum and predicted parameter sets for the simulation of the rainfall experiments. The model efficiency decreased to an acceptable 0.66 when using regionalized macroporosity values and below 0.5 when using regionalized macroporosity values and erosion resistance (Sect. 4.2.1.). These findings are in line with those of Nearing (2006) and Bagarello and Ferro (2012).

Nearing (2006) analyzed the predictability of soil detachment rates on the plot scale by applying the "physical model concept". The idea of this concept is that the best model of an erosion plot is a neighbouring plot with similar properties. Nearing (2006) therefore correlated the erosion rates of neighbouring plots for a large number of experiments and found that the coefficient of determination R^2 reaches a maximum of 0.77. He concluded that no better prediction of soil detachment rates on the plot scale is possible due to the random variability of this natural process on small scales. Bagarello and Ferro (2012) repeated the experiment of Nearing (2006) using data from soil erosion plots in Italy and achieved the same result: the coefficient of determination was below 0.77. This high natural variability on the plot scale is also found within the rainfall simulation experiments carried out in the Weiherbach catchment (Scherer et al., 2012).

Seyfried and Wilcox (1995) proposed that the type of variability of natural data is either stochastic or deterministic, depending on the scale: on the plot scale the variability is stochastic, while it is deterministic on larger scales, such as the catchment scale, because local structures control the response of the system. Kirkby (1998) showed that the deterministic variability on the catchment scale is mainly dependent on the interaction of topography, vegetation and soil type. In the case where the relevant catchment characteristics and structures controlling the response of the system are identified, the spatial and temporal pattern of a state variable can be parameterized by average values, while the small-scale variability can be neglected (Seyfried and Wilcox, 1995; Zehe and Blöschl, 2004). We found that cultivation and tillage operations were the first order control of the erosion resistance for the homogeneous loess soils in the Weiherbach catchment (Scherer et al., 2012). Although the erosion resistance showed a high sensitivity to the simulation results on the plot scale, the spatial and temporal pattern of this parameter was adequately predicted on the catchment scale (Sect. 4.1.3) by using a regionalization approach that represented the dominant control factors.

The spatial and temporal pattern of the macroporosity factor depends on two main influencing factors: (i) the earthworm species in the Weiherbach prefer the Colluvisols at the hill foots which are rich in clay and organic matter (Zehe and Flühler, 2001; van Schaik et al., 2014) leading to higher densities of earthworm borrows in comparison to the calcaric regosols at the hill tops (Sects. 3.2.2 and 4.2.1). This catena related pattern was represented in the model setup by increasing the macroporosity factor from the hill top to the foot (Sect. 3.3.4). (ii) The number of earthworm borrows connected to the surface on intensively cultivated areas varies throughout the year, since the pore system is destroyed by ploughing. After tillage the macropores are rebuilt during the vegetation period by the earthworms (Zehe and Blöschl, 2004). We observed the seasonal variation in macropore connectivity during the calibration of the runoff volume on the plot (Sect. 4.1.1) as well as at catchment scale (Sect. 4.1.3): while the average level of the macroporostiy factors was low during spring, the macroporosity factors reached higher levels at the end of the vegetation period in August and September.

We conclude that all relevant processes and influencing factors for modelling erosion and deposition processes for loess soils on the catchment scale were adequately represented and parameterized in CATFLOW-SED. The validated model setup can be used to shed light on the role of the hillslope form, rainfall intensity, infiltration capacity, land use and tillage practice in erosion scenarios for cultivated loess landscapes. Such scenario analyses are important since heavy storm events are difficult to observe in a specific catchment due to the rareness and the local occurrence of heavy thunderstorms. The capability of the model to analyze land use scenarios was demonstrated by simulating the heaviest observed storm event in the Weiherbach catchment with rearranged land use patterns in a best case and worst case scenario (Sect. 4.2.1). In addition, the model is a useful tool to analyze the risk of particulate substance emissions via erosion and to quantify the effect of mitigation measures.

Future work will focus on the improvement of the predictability of surface runoff simulation. Up to now, the temporal and spatial regionalization of the macroporosity factor dependant on the various land uses and crop types in not yet feasible for the Weiherbach catchment. Zehe et al. (2013) have suggested a promising further approach by using optimality principles to predict the macroporosity of different landscape configurations.

Acknowledgements. The authors acknowledge support by Deutsche Forschungsgemeinschaft and the Open Access Publishing Fund of Karlsruhe Institute of Technology (KIT).

The article processing charges for this open-access publication have been covered by a Research Centre of the Helmholtz Association.

HESSD
12, 3527–3592, 2015

Predicting land use and soil controls on erosion and sediment redistribution

U. Scherer and E. Zehe

Title Page
Abstract | Introduction
Conclusions | References
Tables | Figures
◀| |▶
◀ ▶
Back | Close
Full Screen / Esc
Printer-friendly Version
Interactive Discussion

References

Abrahams, A. D., Li, G., Krishnan, C., and Atkinson, J. F.: A sediment transport equation for interrill overland flow on rough surfaces, Earth Surf. Proc. Land., 26, 1443–1459, doi:10.1002/esp.286, 2001.

Ali, M., Sterk, G., Seeger, M., Boersema, M., and Peters, P.: Effect of hydraulic parameters on sediment transport capacity in overland flow over erodible beds, Hydrol. Earth Syst. Sci., 16, 591–601, doi:10.5194/hess-16-591-2012, 2012.

Ali, M., Seeger, M., Sterk, G., and Moore, D.: A unit stream power based sediment transport function for overland flow, Catena, 101, 197–204, doi:10.1016/j.catena.2012.09.006, 2013.

Alonso, C. V., Neibling, W. H., and Foster, G. R.: Estimating sediment transport capacity in watershed modelling, T. ASAE, 24, 1211–1220, 1981.

Bouraoui, F. and Dillaha, T. A.: ANSWERS-2000: Runoff and sediment transport model, J. Environ. Eng.-ASCE, 122, 493–502, doi:10.1061/(asce)0733-9372(1996)122:6(493), 1996.

Bagarello, V. and Ferro, V.: Testing the “physical model concept” by soil loss data measured in Sicily, Catena, 95, 1–5, 2012.

Bennett, J. P.: Concepts of mathematical modeling of sediment yield, Water Resour. Res., 10, 485–492, 1974.

Beuselinck, L., Govers, G., Steegen, A., Hairsine, P. B., and Poesen, J.: Evaluation of the simple settling theory for predicting sediment deposition by overland flow, Earth Surf. Proc. Land., 24, 993–1007, doi:10.1002/(SICI)1096-9837(199910)24:11<993::AID-ESP24>3.0.CO;2-P, 1999.

Beuselinck, L., Steegen, A., Govers, G., Nachtergaele, J., Takken, I., and Poesen, J.: Characteristics of sediment deposits formed by intense rainfall events in small catchments in the Belgian Loam Belt, Geomorphology, 32, 69–82, 2000.

Beuselinck, L., Govers, G., Hairsine, P. B., Sander, G. C., and Breynaert, M.: The influence of rainfall on sediment transport by overland flow over areas of net deposition, J. Hydrol., 257, 145–163, doi:10.1016/s0022-1694(01)00548-0, 2002.

Beven, K. and Germann, P.: Macropores and water flow in soils, Water Resour. Res., 18, 1311–1325, doi:10.1029/WR018i005p01311, 1982.

Bilotta, G. S. and Brazier, R. E.: Understanding the influence of suspended solids on water quality and aquatic biota, Water Res., 42, 2849–2861, 2008.

Boardman, J.: Soil erosion science: reflections on the limitations of current approaches, Catena, 68, 73–86, 2006.

Boardman, J. and Favis-Mortlock, D.: Modelling Soil Erosion by Water, Springer, Berlin, 1998.

Brazier, R. E., Beven, K. J., Freer, J., and Rowan, J. S.: Equifinality and uncertainty in physically based soil erosion models: application of the GLUE methodology to WEPP – the Water Erosion Prediction Project – for sites in the UK and USA, Earth Surf. Proc. Land., 25, 825–845, doi:10.1002/1096-9837(200008)25:8<825::AID-ESP101>3.0.CO;2-3, 2000.

Brazier, R. E., Beven, K. J., Anthony, S. G., and Rowan, J. S.: Implications of model uncertainty for the mapping of hillslope-scale soil erosion predictions, Earth Surf. Proc. Land., 26, 1333–1352, doi:10.1002/esp.266, 2001.

Cammeraat, E. L. H.: Scale dependent thresholds in hydrological and erosion response of a semi-arid catchment in southeast Spain, Agr. Ecosyst. Environ., 104, 317–332, doi:10.1016/j.agee.2004.01.032, 2004.

Clemens, G. and Stahr, K.: Present and past soil erosion rates in catchments of the Kraichgau area (SW-Germany), Catena, 22, 153–168, doi:10.1016/0341-8162(94)90023-X, 1994.

De Roo, A., Jetten, V., Wesseling, C., and Ritesema, C.: LISEM: a physically-based hydrologic and soil erosion catchment model, in: Modelling Soil Erosion by Water, NATO ASI Series I: Global Environmental Change, Vol. 55, edited by: Boardman, J. and Favis-Mortlock, D., Springer, Berlin, 429–440, 1998.

Engelund, F. and Hansen, E.: A Monograph on Sediment Transport in Alluvial Streams, Teknisk Forlag, Copenhagen, 1967.

Engman, E. T.: Roughness coefficients for routing surface runoff, J. Irrig. Drain. E.-ASCE, 112, 39–53, 1986.

Everaert, W.: Empirical relations for the sediment transport capacity of interrill flow, Earth Surf. Proc. Land., 16, 513–532, doi:10.1002/esp.3290160604, 1991.

Ferro, V.: Evaluating overland flow sediment transport capacity, Hydrol. Process., 12, 1895–1910, 1998.

Foster, G. R.: Modeling the erosion process, in: Hydrologic Modeling of Small Watersheds, ASAE Monograph No. 5, edited by: Haan, C. T., Johnseon, H. P., and Brakensiek, D. L., American Society of Agricultural Engineers, St. Joseph, Michigan, USA, 297–382, 1982.

Foster, G. R. and Meyer, L. D.: A closed form soil erosion equation for upland areas, in: Sedimentation, Symposium to Honor Professor H. A. Einstein, edited by: Shen, H. W., Fort Collins, Colorado, USA, 1972.

Foster, G. R. and Meyer, L. D.: Mathematical simulation of upland erosion by fundamental erosion mechanics, ARS-S-40, USDA-Agricultural Research Services, Oxford, Missouri, USA, 190–207, 1975.
Fuchs, S. and Schwarz, M.: Ableitung bodenspezifischer Anreicherungsfaktoren zur Bestimmung des Phosphor- und Schwermetalleintrages in Oberflächengewässer durch Erosion, Abschlussbericht BWPLUS, Vorhabensnummer BWR 24017, Institute of Water and River Basin Management, University Karlsruhe, Karlsruhe, Germany, 2007.
Gerlinger, K.: Erosionsprozesse auf Lößböden: Experimente und Modellierung, Institute for Water and River Basin Management, University Karlsruhe, Karlsruhe, 1997.
Gerlinger, K. and Scherer, U.: Simulating soil erosion and phosphorus transport on loess soils using advanced hydrological and erosional models, modelling soil erosion, sediment transport and closely related hydrological processes, in: Proceedings of a Symposium held at Vienna, July 1998, Vienna, 119–127, 1998.
Giménez, R. and Govers, G.: Interaction between bed roughness and flow hydraulics in eroding rills, Water Resour. Res., 37, 791–799, 2001.
Giménez, R. and Govers, G.: Flow detachment by concentrated flow on smooth and irregular beds, Soil Sci. Soc. Am. J., 66, 1475–1483, 2002.
Govers, G.: Evaluation of transporting capacity formulae for overland flow, in: Overland Flow, Hydraulics and Erosion Mechanics, edited by: Parsons, A. J. and Abrahams, A. D., UCL Press, London, 243–273, 1992.
Govers, G. and Rauws, G.: Transporting capacity of overland flow on plane and irregular beds, Earth Surf. Proc. Land., 11, 515–524, 1986.
Govers, G., Takken, I., and Helming, K.: Soil roughness and overland flow, Agronomie, 20, 131–146, 2000.
Govers, G., Giménez, R., and Van Oost, K.: Rill erosion: exploring the relationship between experiments, modelling and field observations, Earth-Sci. Rev., 84, 87–102, 2007.
Graeff, T., Zehe, E., Reusser, D., Lück, E., Schröder, B., Wenk, G., John, H., and Bronstert, A.: Process identification through rejection of model structures in a mid-mountainous rural catchment: observations of rainfall–runoff response, geophysical conditions and model inter-comparison, Hydrol. Process., 23, 702–718, doi:10.1002/hyp.7171, 2009.
Guy, B. T., Dickenson, W. T., Sohrabi, T. M., and Rudra, R. P.: Development of an empirical model for calculating sediment-transport capacity in shallow overland flows: model calibration, Biosyst. Eng., 103, 245–255, doi:10.1016/j.biosystemseng.2009.02.013, 2009a.

HESSD
12, 3527–3592, 2015

Guy, B. T., Rudra, R. P., Dickenson, W. T., and Sohrabi, T. M.: Empirical model for calculating sediment-transport capacity in shallow overland flows: model development, Biosyst. Eng., 103, 105–115, doi:10.1016/j.biosystemseng.2009.02.002, 2009b.

Haan, C. T., Barfield, B. J., and Hayes, J. C.: Design Hydrology and Sedimentology For Small Catchments, Academic Press, San Diego, USA, 1994.

Hahn, H. H. and Beudert, G.: Schlussbericht des BMBF-Verbundprojektes "Prognosemodell für die Gewässerbelastung durch Stofftransport aus kleinen ländlichen Einzugsgebieten" – Weiherbachprojekt, Teilprojekt 8: Stofftransport und Bilanzierung von Nährstoffen. Untersuchung des Stoffaustrages unter besonderer Berücksichtigung der Abspülung von befestigten landwirtschaftlichen Flächen, Institut für Siedlungswasserwirtschaft der Universität Karlsruhe (TH), Karlsruhe, 1997.

Hairsine, P. B. and Rose, C. W.: Modeling water erosion due to overland flow using physical principles, 2. Rill flow, Water Resour. Res., 28, 245–250, 1992a.

Hairsine, P. B. and Rose, C. W.: Modeling water erosion due to overland flow using physical principles, 1. Sheet flow, Water Resour. Res., 28, 237–243, 1992b.

Harmon, R. S. and Doe, W. W.: Landscape Erosion and Evolution Modeling, Kluwer Academic/Plenum Publishers, New York, 2001.

Heatwole, C. D., Zacharias, S., and Workman, S. R.: OPUS: model description and evaluation, Paper No. 98-2201, ASAE Meeting Presentation, ASAE, St. Joseph, USA, 1998.

Hessel, R.: Consequences of hyperconcentrated flow for process-based soil erosion modelling on the Chinese Loess Plateau, Earth Surf. Proc. Land., 31, 1100–1114, doi:10.1002/esp.1307, 2006.

Hessel, R. and Jetten, V.: Suitability of transport equations in modelling soil erosion for a small Loess Plateau catchment, Eng. Geol., 91, 56–71, doi:10.1016/j.enggeo.2006.12.013, 2007.

Huang, C.: Empirical analysis of slope and runoff for sediment delivery from interrill areas, Soil Sci. Soc. Am. J., 59, 982–990, 1995.

Huang, C.-H., Laflen, J. M., and Bradford, J. M.: Evaluation of the detachment-transport coupling concept in the WEPP Rill Erosion equation, Soil Sci. Soc. Am. J., 60, 734–739, doi:10.2136/sssaj1996.03615995006000030008x, 1996.

Jackisch, C., Zehe, E., Samaniego, L., and Singh, A. K.: An experiment to gauge an ungauged catchment: rapid data assessment and eco-hydrological modelling in a data-scarce rural catchment, Hydrol. Sci. J.-J. Sci. Hydrol., 59, 2103–2125, doi:10.1080/02626667.2013.870662, 2014.

HESSD

12, 3527–3592, 2015

Predicting land use and soil controls on erosion and sediment redistribution

U. Scherer and E. Zehe

Jayawardena, A. W. and Bhuiyan, R. R.: Evaluation of an interrill soil erosion model using laboratory catchment data, Hydrol. Process., 13, 89–100, 1999.
Jetten, V. and Favis-Mortlock, D.: Modelling soil erosion in Europe, in: Soil Erosion in Europe, edited by: Boardman, J. and Poesen, J., Wiley & Sons, Chichester, 695–716, 2006.
Jetten, V., Govers, G., and Hessel, R.: Erosion models: quality of spatial predictions, Hydrol. Process., 17, 887–900, 2003.
Johnson, B. E., Julien, P. Y., Molnar, D. K., and Watson, C. C.: The two-dimensional upland erosion model CASC2D-SED, J. Am. Water Resour. As., 36, 31–42, 2000.
Julien, P. Y. and Simons, D. B.: Sediment transport capacity of overland flow, T. ASAE, 28, 755–762, 1985.
Kazanskij, J.: Zur Turbulenzstruktur von Feststoff-Wasser-Gemischen in Rohrleitungen, TH Hannover, Hannover, 1972.
Kinnell, P. I. A.: Raindrop-impact-induced erosion processes and prediction: a review, Hydrol. Process., 19, 2815–2844, 2005.
Kirkby, M.: Modelling across scales: the MEDALUS family of models, in: Modelling Soil Erosion by Water, edited by: Boardman, J. and Favis-Mortlock, D., Springer, Berlin, 161–173, 1998.
Klaus, J. and Zehe, E.: Modelling rapid flow response of a tile-drained field site using a 2D physically based model: assessment of “equifinal” model setups, Hydrol. Process., 24, 1595–1609, doi:10.1002/hyp.7687, 2010.
Klaus, J. and Zehe, E.: A novel explicit approach to model bromide and pesticide transport in connected soil structures, Hydrol. Earth Syst. Sci., 15, 2127–2144, doi:10.5194/hess-15-2127-2011, 2011.
Kleidon, A., Zehe, E., Ehret, U., and Scherer, U.: Thermodynamics, maximum power, and the dynamics of preferential river flow structures at the continental scale, Hydrol. Earth Syst. Sci., 17, 225–251, doi:10.5194/hess-17-225-2013, 2013.
Knapen, A., Poesen, J., Govers, G., Gyssels, G., and Nachtergaele, J.: Resistance of soils to concentrated flow erosion: a review, Earth-Sci. Rev., 80, 75–109, doi:10.1016/j.earscirev.2006.08.001, 2007.
Knisel, W. G.: CREAMS, a Field Scale Model for Chemicals, Runoff, and Erosion from Agricultural Management Systems, Conservation Report No. 26, United States Department of Agriculture, Washington, D.C., USA, 1980.
Kronvang, B., Vagstad, N., Behrendt, H., Bogestrand, J., and Larsen, S. E.: Phosphorus losses at the catchment scale within Europe: an overview, Soil Use Manage., 23, 104–116, 2007.

HESSD
12, 3527–3592, 2015

Predicting land use and soil controls on erosion and sediment redistribution

U. Scherer and E. Zehe

Title Page
Abstract Introduction
Conclusions References
Tables Figures
◀ ▶
Back Close
Full Screen / Esc
Printer-friendly Version
Interactive Discussion

Lei, T. W., Nearing, M. A., Haghighi, K., and Bralts, V. F.: Rill erosion and morphological evolution: a simulation model, Water Resour. Res., 34, 3157–3168, doi:10.1029/98WR02162, 1998.
Lei, T. W., Zhang, Q. W., Zhao, J., and Nearing, M. A.: Tracing sediment dynamics and sources in eroding rills with rare earth elements, Eur. J. Soil Sci., 57, 287–294, doi:10.1111/j.1365-2389.2005.00737.x, 2006.
Lesschen, J. P., Schoorl, J. M., and Cammeraat, L. H.: Modelling runoff and erosion for a semi-arid catchment using a multi-scale approach based on hydrological connectivity, Geomorphology, 109, 174–183, 2009.
Li, G. and Abrahams, A. D.: Controls of sediment transport capacity in laminar interrill flow on stone-covered surfaces, Water Resour. Res., 35, 305–310, doi:10.1029/98wr02534, 1999.
Li, W. J., Li, D. X., and Wang, X. K.: An approach to estimating sediment transport capacity of overland flow, Sci. China Ser E, 54, 2649–2656, doi:10.1007/s11431-011-4506-x, 2011.
Maurer, T.: Physikalisch begründete zeitkontinuierliche Modellierung des Wassertransportes in kleinen ländlichen Einzugsgebieten, Institute of Hydrology and Water Resources Management, University Karlsruhe, Karlsruhe, Germany, 1997.
Merten, G. H., Nearing, M. A., and Borges, A. L. O.: Effect of sediment load on soil detachment and deposition in rills, Soil Sci. Soc. Am. J., 65, 861–868, doi:10.2136/sssaj2001.653861x, 2001.
Meyer, L. D. and Wischmeier, W. H.: Mathematical simulation of the process of soil erosion by water, T. ASAE, 12, 754–758, 1969.
Morgan, R. P. C. and Quinton, J. N.: Erosion modelling, in: Landscape Erosion and Evolution Modeling, edited by: Hammon, R. S. and Doe, W. W., Kluwer Academic/Plenum Publishers, New York, 117–143, 2001.
Morgan, R. P. C., Quinton, J. N., Smith, R. E., Govers, G., Poesen, J., Chisci, G., and Torri, D.: The EUROSEM model, in: Modelling Soil Erosion by Water, NATO ASI Series I: Global Environmental Change, Vol. 55, edited by: Boardman, J. and Favis-Mortlock, D., Springer, Berlin, 389–398, 1998.
Mualem, Y.: New model for predicting hydraulic conductivity of unsaturated porous media, Water Resour. Res., 12, 513–522, doi:10.1029/WR012i003p00513, 1976.
Nadeu, E., de Vente, J., Martinez-Mena, M., and Boix-Fayos, C.: Exploring particle size distribution and organic carbon pools mobilized by different erosion processes at the catchment scale, J. Soil Sediment., 11, 667–678, doi:10.1007/s11368-011-0348-1, 2011.

HESSD
12, 3527–3592, 2015

Predicting land use and soil controls on erosion and sediment redistribution

U. Scherer and E. Zehe

Nash, J. E. and Sutcliffe, J. V.: River flow forecasting through conceptual models part I – A discussion of principles, J. Hydrol., 10, 282–290, 1970.
Nearing, M. A.: Can soil erosion be predicted?, in: Soil Erosion and Sediment Redistribution in River Catchments, edited by: Owens, P. N. and Collins, A. J., CABI Publishing, Wallingford, 145–152, 2006.
Nearing, M. A., Lane, L. J., Alberts, E. E., and Laflen, J. M.: Prediction technology for soil erosion by water: status and research needs, Soil Sci. Soc. Am. J., 54, 1702–1711, doi:10.2136/sssaj1990.03615995005400060033x, 1990.
Nearing, M. A., Norton, L. D., Bulgakov, D. A., Larionov, G. A., West, L. T., and Dontsova, K. M.: Hydraulics and erosion in eroding rills, Water Resour. Res., 33, 865–876, 1997.
Nord, G. and Esteves, M.: Evaluation of sediment transport formulae and detachment parameters in eroding rills using PSEM_2D and the Water Erosion Prediction Project (WEPP) database, Water Resour. Res., 43, W08420, doi:10.1029/2006wr005444, 2007.
Nord, G., Esteves, M., Lapetite, J.-M., and Hauet, A.: Effect of particle density and inflow concentration of suspended sediment on bedload transport in rill flow, Earth Surf. Proc. Land., 34, 253–263, doi:10.1002/esp.1710, 2009.
Owens, P. N., Batalla, R. J., Collins, A. J., Gomez, B., Hicks, D. M., Horowitz, A. J., Kondolf, G. M., Marden, M., Page, M. J., Peacock, D. H., Petticrew, E. L., Salomons, W., and Trustrum, N. A.: Fine-grained sediment in river systems: environmental significance and management issues, River Res. Appl., 21, 693–717, doi:10.1002/rra.878, 2005.
Paik, K. and Kumar, P.: Optimality approaches to describe characteristic fluvial patterns on landscapes, Philos. T. Roy. Soc. B, 365, 1387–1395, doi:10.1098/rstb.2009.0303, 2010.
Plate, E. J. and Zehe, E.: Hydrologie und Stoffdynamik kleiner Einzugsgebiete, Prozesse und Modelle, Schweizerbart, Stuttgart, 2008.
Prosser, I. P. and Rustomji, P.: Sediment transport relations for overland flow, Prog. Phys. Geogr., 24, 179–193, 2000.
Rejman, J. and Iglik, I.: Topsoil reduction and cereal yields on loess soils of southeast Poland, Land Degrad. Dev., 21, 401–405, doi:10.1002/ldr.963, 2010.
Salles, C., Poesen, J., and Govers, G.: Statistical and physical analysis of soil detachment by raindrop impact: rain erosivity indices and threshold energy, Water Resour. Res., 36, 2721–2729, doi:10.1029/2000wr900024, 2000.

HESSD
12, 3527–3592, 2015

Predicting land use and soil controls on erosion and sediment redistribution

U. Scherer and E. Zehe

Schäfer, D.: Bodenhydraulische Eigenschaften eines Kleineinzugsgebietes – Vergleich und Bewertung unterschiedlicher Verfahren, Institute for Hydromechanics, University Karlsruhe, Karlsruhe, Germany, 1999.

Scherer, U., Zehe, E., Träbing, K., and Gerlinger, K.: Prediction of soil detachment in agricultural loess catchments: model development and parameterisation, Catena, 90, 63–75, doi:10.1016/j.catena.2011.11.003, 2012.

Schmidt, J.: Entwicklung und Anwendung eines physikalisch begründeten Simulationsmodells für die Erosion geneigter landwirtschaftlicher Nutzflächen, Berliner Geographische Abhandlungen 61, Institute of Geographical Sciences, Freie Universität Berlin, Berlin, Germany, 1996.

Schmidt, J., Werner, M. V., and Michael, A.: Application of the EROSION 3D model to the CATSOP watershed, the Netherlands, Catena, 37, 449–456, 1999.

Seibert, S., Auerswald, K., Fiener, P., Disse, M., Martin, W., Haider, J., Michael, A., and Gerlinger, K.: Surface runoff from arable land – a homogenized data base of 726 rainfall simulation experiments, CRC/TR32 Database (TR32DB), doi:10.1594/GFZ.TR32.2, 2011.

Seyfried, M. S. and Wilcox, B. P.: Scale and the nature of spatial variability: field examples having implications for hydrologic modeling, Water Resour. Res., 31, 173–184, 1995.

Smith, R. E., Goodrich, D. C., and Quinton, J. N.: Dynamic, distributed simulation of watershed erosion: the KINEROS2 and EUROSEM models, J. Soil Water Conserv., 50, 517–520, 1995.

Takken, I., Beuselinck, L., Nachtergaele, J., Govers, G., Poesen, J., and Degraer, G.: Spatial evaluation of a physically-based distributed erosion model (LISEM), Catena, 37, 431–447, 1999.

Tayfur, G.: Applicability of sediment transport capacity models for nonsteady state erosion from steep slopes, J. Hydrol. Eng., 7, 252–259, 2002.

van Genuchten, M. T.: A closed-form equation for predicting the hydraulic conductivity of unsaturated soils, Soil Sci. Soc. Am. J., 44, 892–898, doi:10.2136/sssaj1980.03615995004400050002x, 1980.

Van Oost, K., Govers, G., Cerdan, O., Thauré, D., Van Rompaey, A., Steegen, A., Nachtergaele, J., Takken, I., and Poesen, J.: Spatially distributed data for erosion model calibration and validation: the Ganspoel and Kinderveld datasets, Catena, 61, 105–121, doi:10.1016/j.catena.2005.03.001, 2005.

van Schaik, L., Palm, J., Klaus, J., Zehe, E., and Schroder, B.: Linking spatial earthworm distribution to macropore numbers and hydrological effectiveness, Ecohydrology, 7, 401–408, doi:10.1002/eco.1358, 2014.
Verheijen, F. G. A., Jones, R. J. A., Rickson, R. J., and Smith, C. J.: Tolerable versus actual soil erosion rates in Europe, Earth-Sci. Rev., 94, 23–38, doi:10.1016/j.earscirev.2009.02.003, 2009.
Wainwright, J., Turnbull, L., Ibrahim, T. G., Lexartza-Artza, I., Thornton, S. F., and Brazier, R. E.: Linking environmental régimes, space and time: interpretations of structural and functional connectivity, Geomorphology, 126, 387–404, doi:10.1016/j.geomorph.2010.07.027, 2011.
Walling, D. E.: Human impact on land–ocean sediment transfer by the world's rivers, Geomorphology, 79, 192–216, 2006.
Wan, Z. and Wang, Z.: Hyperconcentrated Flow, IAHR Monograph, AA Balkema Publishers, Rotterdam, 1994.
USDA – United States Department of Agriculture: Water Erosion Prediction Project (WEPP), Technical Documentation, NSERL Report No. 10, National Soil Erosion Research Laboratory, West Lafayette, Indiana, USA, 1995, available at: http://www.ars.usda.gov/Research/docs.htm?docid=18073, last access: 30 March 2015.
Wicks, J. M. and Bathurst, J. C.: SHESED: a physically based, distributed erosion and sediment yield component for the SHE hydrological modelling system, J. Hydrol., 175, 213–238, 1996.
Wienhöfer, J. and Zehe, E.: Predicting subsurface stormflow response of a forested hillslope – the role of connected flow paths, Hydrol. Earth Syst. Sci., 18, 121–138, doi:10.5194/hess-18-121-2014, 2014.
Winteraeken, H. J. and Spaan, W. P.: A new approach to soil erosion and runoff in south Limburg – the Netherlands, Land Degrad. Dev., 21, 346–352, doi:10.1002/ldr.1009, 2010.
Yalin, M. S.: Mechanics of Sediment Transport, Pergamon Press, Oxford, England, 1972.
Yang, C. T.: Incipient motion and sediment transpor, J. Hydrol. Eng. Div.-ASCE, 99, 1679–1703, 1973.
Yu, B.: A unified framework for water erosion and deposition equations, Soil Sci. Soc. Am. J., 67, 251–257, doi:10.2136/sssaj2003.2510, 2003.
Zehe, E.: Stofftransport in der ungesättigten Bodenzone auf verschiedenen Skalen, Institute of Hydrology and Water Resources Management, University Karlsruhe, Karlsruhe, Germany, 1999.

HESSD
12, 3527–3592, 2015

Zehe, E. and Blöschl, G.: Predictability of hydrologic response at the plot and catchment scales: role of initial conditions, Water Resour. Res., 40, W10202, doi:10.1029/2003wr002869, 2004.

Zehe, E. and Flühler, H.: Slope scale variation of flow patterns in soil profiles, J. Hydrol., 247, 116–132, doi:10.1016/s0022-1694(01)00371-7, 2001.

Zehe, E. and Sivapalan, M.: Threshold behaviour in hydrological systems as (human) geo-ecosystems: manifestations, controls, implications, Hydrol. Earth Syst. Sci., 13, 1273–1297, doi:10.5194/hess-13-1273-2009, 2009.

Zehe, E., Maurer, T., Ihringer, J., and Plate, E.: Modeling water flow and mass transport in a loess catchment, Phys. Chem. Earth Pt. B, 26, 487–507, 2001.

Zehe, E., Becker, R., Bárdossy, A., and Plate, E.: Uncertainty of simulated catchment runoff response in the presence of threshold processes: role of initial soil moisture and precipitation, J. Hydrol., 315, 183–202, doi:10.1016/j.jhydrol.2005.03.038, 2005.

Zehe, E., Elsenbeer, H., Lindenmaier, F., Schulz, K., and Blöschl, G.: Patterns of predictability in hydrological threshold systems, Water Resour. Res., 43, W07434, doi:10.1029/2006WR005589, 2007.

Zehe, E., Ehret, U., Blume, T., Kleidon, A., Scherer, U., and Westhoff, M.: A thermodynamic approach to link self-organization, preferential flow and rainfall–runoff behaviour, Hydrol. Earth Syst. Sci., 17, 4297–4322, doi:10.5194/hess-17-4297-2013, 2013.

Zhang, G.-H., Liu, Y.-M., Han, Y.-F., and Zhang, X. C.: Sediment transport and soil detachment on steep slopes: I. Transport capacity estimation, Soil Sci. Soc. Am. J., 73, 1291–1297, doi:10.2136/sssaj2008.0145, 2009a.

Zhang, G. H., Tang, M. K., and Zhang, X. C.: Temporal variation in soil detachment under different land uses in the Loess Plateau of China, Earth Surf. Proc. Land., 34, 1302–1309, doi:10.1002/esp.1827, 2009b.

Zhang, G. H., Wang, L. L., Tang, K. M., Luo, R. T., and Zhang, X. C.: Effects of sediment size on transport capacity of overland flow on steep slopes, Hydrol. Sci. J.-J. Sci. Hydrol., 56, 1289–1299, doi:10.1080/02626667.2011.609172, 2011.

HESSD

12, 3527–3592, 2015

Table 1. Soil hydraulic properties after van Genuchten–Mualem (van Genuchten, 1980; Mualem, 1976). Where k_s is saturated hydraulic conductivity, θ_s porosity, θ_r residual water content, α air entry value and n shape parameter.

Soil type	k_s direct $m\,s^{-1}$	θ_s $m^3\,m^{-3}$	θ_r $m^3\,m^{-3}$	α m^{-1}	n –
Calcaric Regosol	2.1×10^{-6}	0.44	0.06	0.40	2.06
	$\pm0.9\times10^{-6}$	±0.1	±0.1	±0.03	±0.08
Colluvisol	5.0×10^{-6}	0.40	0.04	1.90	1.25
	$\pm0.2\times10^{-5}$	±0.05	±0.12	±0.20	±0.001

HESSD
12, 3527–3592, 2015

Table 2. Percentage of land use in the Weiherbach catchment for the main crop periods of 1994 and 1995.

Land use	1994	1995
Grain/vegetables	122 ha (34.7 %)	152 ha (43.4 %)
Corn	55 ha (15.7 %)	42 ha (12.1 %)
Fodder/sugar beet	24 ha (6.9 %)	19 ha (5.3 %)
Sun flower	43 ha (12.4 %)	27 ha (7.7 %)
Grass land/forest/sealed area	106 ha (30.3 %)	110 ha (31.6 %)

HESSD
12, 3527–3592, 2015

Table 3. Cumulative rainfall as well as discharge volume and sediment load balanced at gauge Menzingen for three heavy erosion events in the Weiherbach catchment.

Date of the event	cumulative rainfall mm	discharge volume m^3	peak flow $m^3\,s^{-1}$	sediment load t
27 Jun 1994	78.6[a]	32 682	7.92	1815
12 Aug 1994	34.4[b]	3699	1.00	35
13 Aug 1995	73.6[a]	20 376	3.17	607

[a] Measured at rainfall gauge WB0, [b] measured at rainfall gauge WB1.

HESSD
12, 3527–3592, 2015

Predicting land use and soil controls on erosion and sediment redistribution

U. Scherer and E. Zehe

HESSD
12, 3527–3592, 2015

Predicting land use and soil controls on erosion and sediment redistribution

U. Scherer and E. Zehe

Table 4. Mean percentages of grain size fractions for the main soil textures in the Weiherbach catchment.

Soil texture in %	clay	silt fine	middle	coarse	sand finest	fine	middle	coarse
Silty loam	27.6	7.7	21.7	35.9	2.4	0.7	1.8	2.2
Loamy silt	14.6	6.0	23.9	51.0	2.5	0.4	1.1	0.5
Very loamy silt	21.7	6.7	23.0	45.7	1.8	0.3	0.6	0.2
Clayey loam	37.0	13.5	14.6	20.8	2.6	1.6	4.2	5.7
Loamy clay	51.0	11.4	13.9	17.5	2.1	1.0	1.5	1.5

HESSD
12, 3527–3592, 2015

Predicting land use and soil controls on erosion and sediment redistribution

U. Scherer and E. Zehe

Table 5. Results of the regression analysis between calibrated macroporosity factors f_m and soil properties (clay content CC, organic matter OM and initial soil moisture θ) of the irrigation plots for 39 rainfall simulation experiments carried out in two intensity measuring campaigns in spring and late summer.

Sample	Clay content (CC) %	Organic matter (OM) %	Soil moisture (θ) Vol.-%
All experiments (n = 39)	$f_m = 0.16 \times CC - 0.86$ $R^2 = 0.46$	$f_m = 1.33 \times OM + 0.21$ $R^2 = 0.13$	$f_m = -0.03 \times \theta + 3.03$ $R^2 = 0.02$
Spring experiments (n = 20)	$f_m = 0.17 \times CC - 1.63$ $R^2 = 0.66$	$f_m = 1.75 \times OM + 1.06$ $R^2 = 0.13$	$f_m = 0.17 \times \theta - 1.60$ $R^2 = 0.17$
Summer experiments (n = 19)	$f_m = 0.17 \times CC - 0.54$ $R^2 = 0.51$	$f_m = 1.50 \times OM + 0.44$ $R^2 = 0.11$	$f_m = 0.14 \times \theta + 1.54$ $R^2 = 0.14$

Table 6. Comparison of observed and modelled sediment volumes at gauge Menzingen for three heavy storm events.

Date of the event	sediment volume observed in t	sediment volume modelled in t	variation %
27 Jun 1994	1815	1949	+7.4
12 Aug 1994	35	37	+5.7
13 Aug 1995	607	630	+3.8

HESSD
12, 3527–3592, 2015

Table 7. Goodness of fit measures for the comparison of observed and modelled cumulative runoff and detachment rates of 39 rainfall simulation experiments for different combinations of specific and predicted values for the model parameters macroporosity factor f_m and erosion resistance f_{crit}. Where RMSE is root mean square error and E model efficiency (Nash and Sutcliffe, 1970).

Combination	f_{crit}: specific		f_{crit}: predicted	
f_m: specific	runoff:	$E = 0.97$, RMSE = 0.04 m^3	runoff:	same as before
	detachment:	$E = 0.95$, RMSE = 11.0 kg	detachment:	$E = 0.56$, RMSE = 31.9 kg
f_m: predicted	runoff:	$E = 0.66$, RMSE = 0.13 m^3	runoff:	same as before
	detachment:	$E = 0.79$, RMSE = 22.8 kg	detachment:	$E = 0.46$, RMSE = 35.4 kg

HESSD
12, 3527–3592, 2015

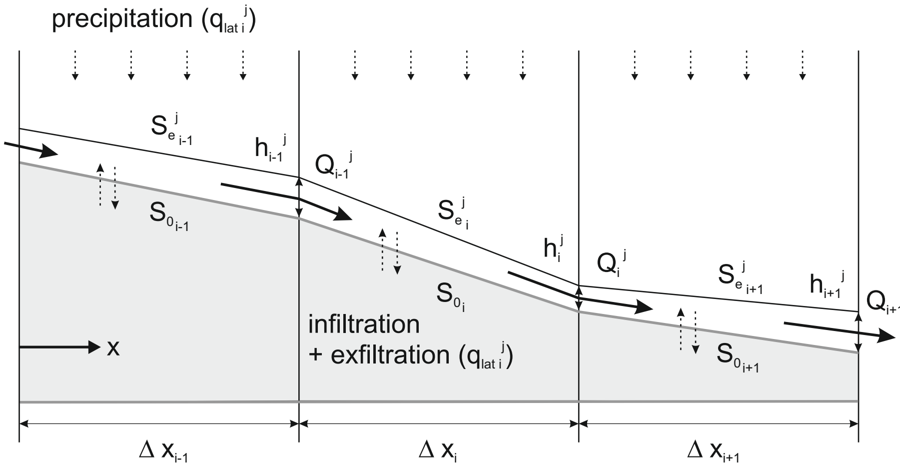

Figure 1. Scheme for overland flow modeling in CATFLOW-SED according to the diffusive wave procedure. Where S_0 is gradient of the discretization element, S_e gradient of the water level, h flow depth in m, Q discharge in $m^3\,s^{-1}$, q_{lat} is lateral inflow by precipitation and infiltration/exfiltration in $m^2\,s^{-1}$, x length coordinate in m, Δx length of discretization element in m, i index of discretization element, j index of time step.

HESSD
12, 3527–3592, 2015

Predicting land use and soil controls on erosion and sediment redistribution

U. Scherer and E. Zehe

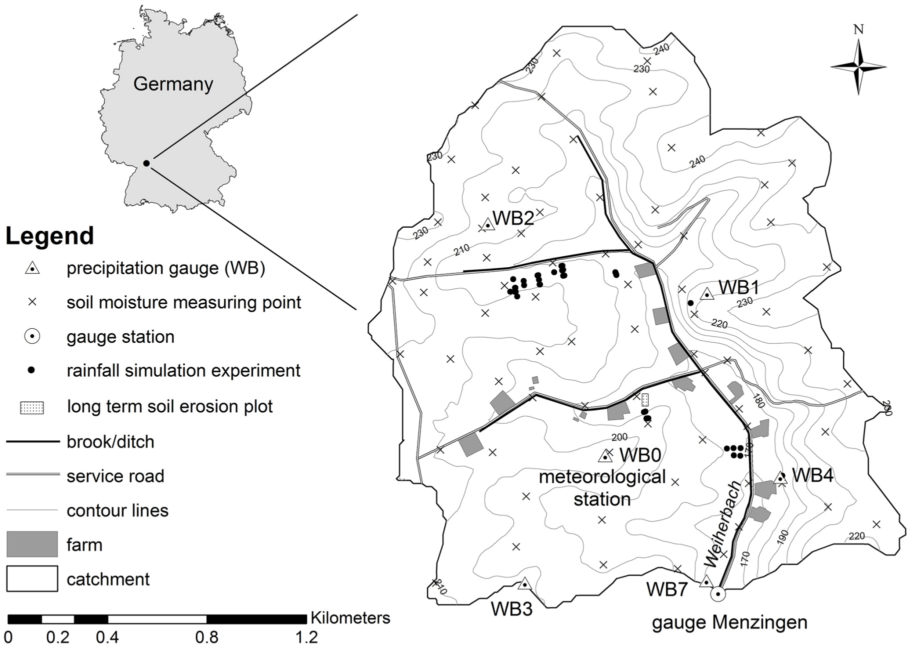

Figure 2. Instrumentation of the Weiherbach catchment and location of rainfall simulation experiments.

HESSD
12, 3527–3592, 2015

Predicting land use and soil controls on erosion and sediment redistribution

U. Scherer and E. Zehe

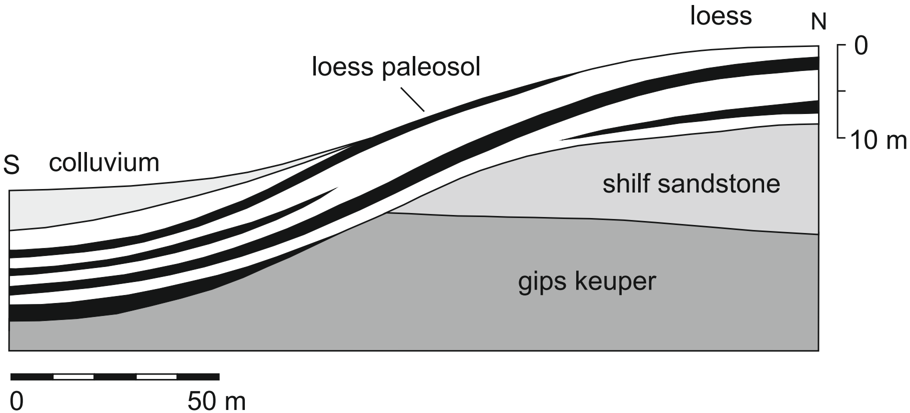

Figure 3. Geological cross-section of a typical hillslope in the Weiherbach catchment.

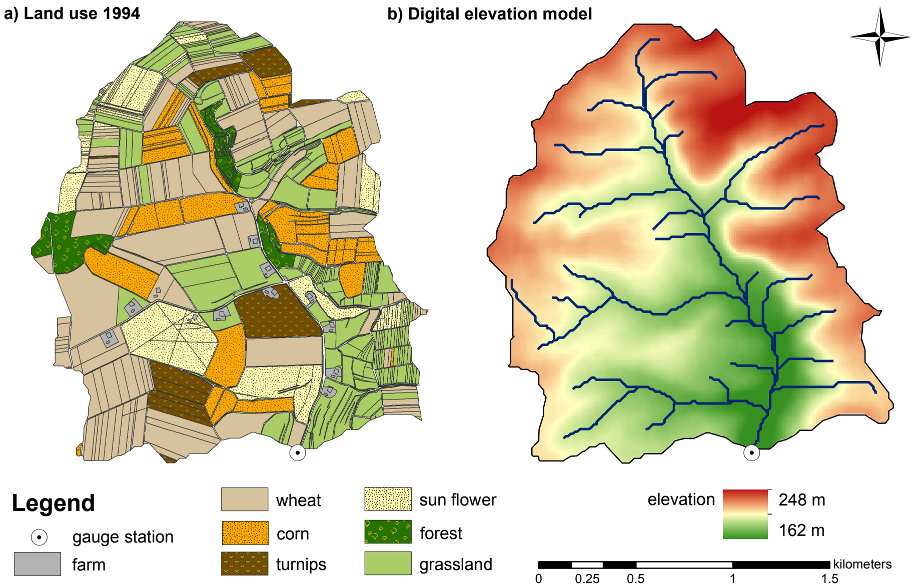

Figure 4. (a) Land use pattern during the main crop period in 1994 and **(b)** digital elevation model of the Weiherbach catchment.

HESSD
12, 3527–3592, 2015

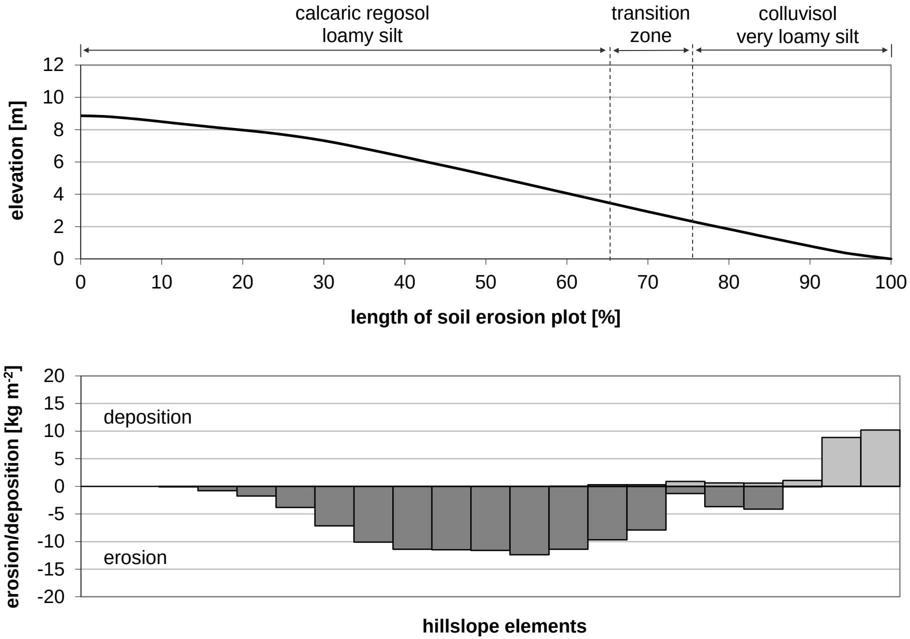

Figure 5. Model setup and simulation results for the long-term soil erosion plot in the Weiherbach catchment. Top panel: Cross-section of the soil erosion plot and assignment of soil textures. Bottom panel: Simulation results of cumulative erosion and deposition rates for the storm event on 27 June 1994.

HESSD
12, 3527–3592, 2015

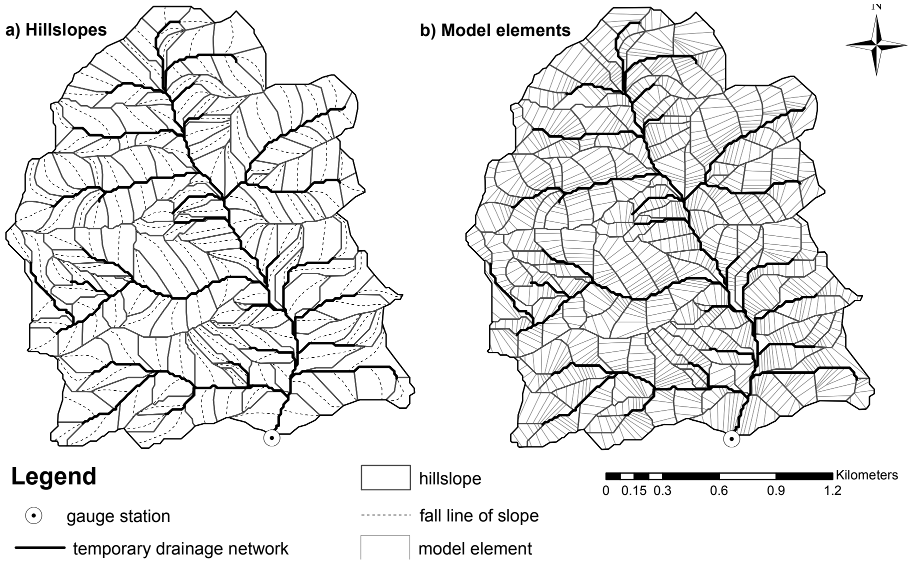

Figure 6. Discretization of the catchment area in hillslopes, drainage network and modelling elements. **(a)** Topview on hillslopes and fall lines of slopes. **(b)** Topview on model elements.

HESSD
12, 3527–3592, 2015

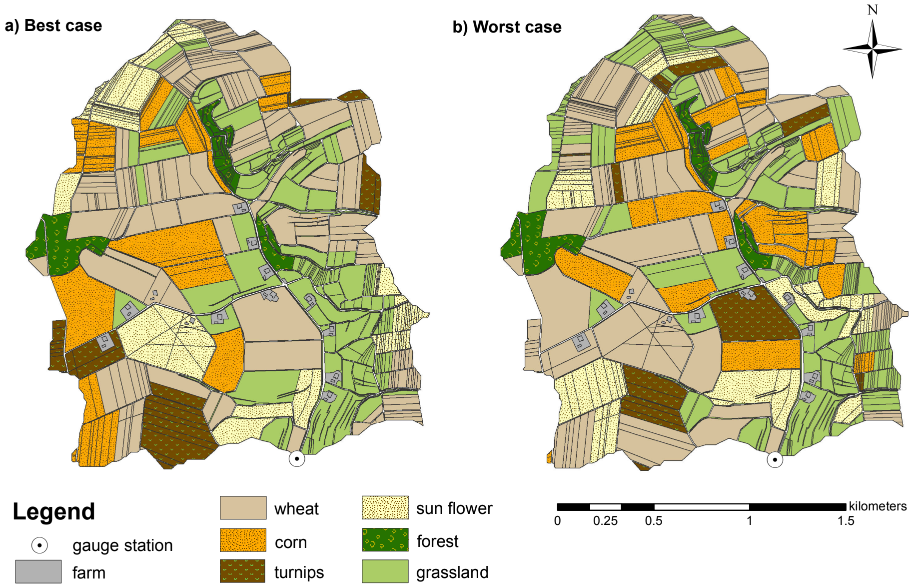

Figure 7. Land use pattern for **(a)** "best case" and **(b)** "worst case" scenarios in the Weiherbach catchment.

HESSD
12, 3527–3592, 2015

Predicting land use and soil controls on erosion and sediment redistribution

U. Scherer and E. Zehe

Title Page
Abstract Introduction
Conclusions References
Tables Figures
◀I ▶I
◀ ▶
Back Close
Full Screen / Esc
Printer-friendly Version
Interactive Discussion

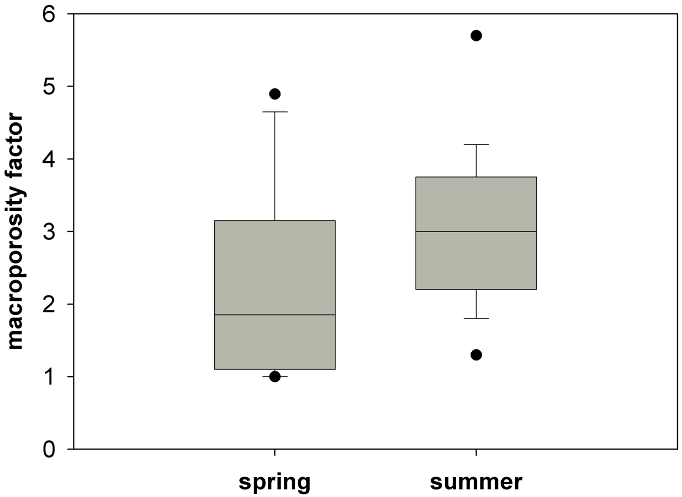

Figure 8. Variation of the calibrated macroporosity factors for the rainfall simulation experiments carried out during two intensity measuring campaigns in spring (20 experiments) and late summer (19 experiments).

HESSD
12, 3527–3592, 2015

Predicting land use and soil controls on erosion and sediment redistribution

U. Scherer and E. Zehe

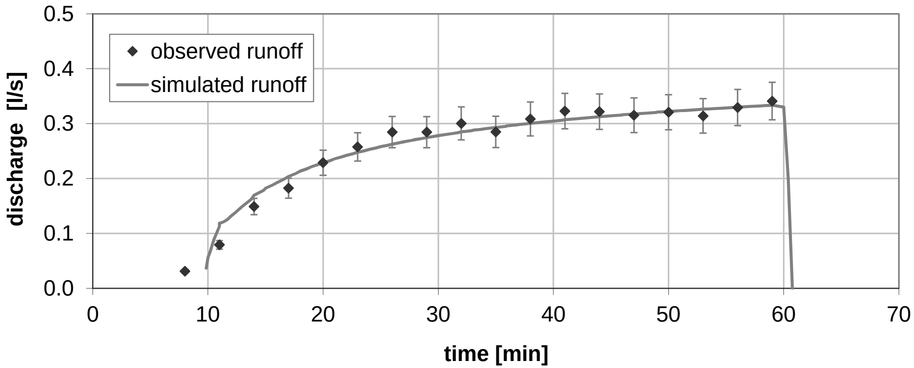

Figure 9. Comparison of observed and simulated surface runoff for a rainfall simulation experiment carried out in the Weiherbach catchment on 30 March 1994.

HESSD
12, 3527–3592, 2015

Predicting land use and soil controls on erosion and sediment redistribution

U. Scherer and E. Zehe

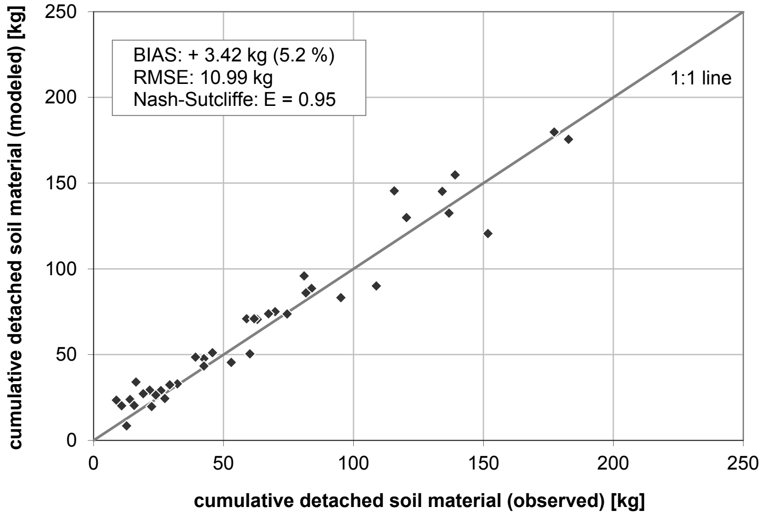

Figure 10. Comparison of observed and modelled cumulative detachment rates of 39 rainfall simulation experiments. Where BIAS is systematic error, RMSE root mean square error and *E* model efficiency (Nash and Sutcliffe, 1970).

HESSD
12, 3527–3592, 2015

Predicting land use and soil controls on erosion and sediment redistribution

U. Scherer and E. Zehe

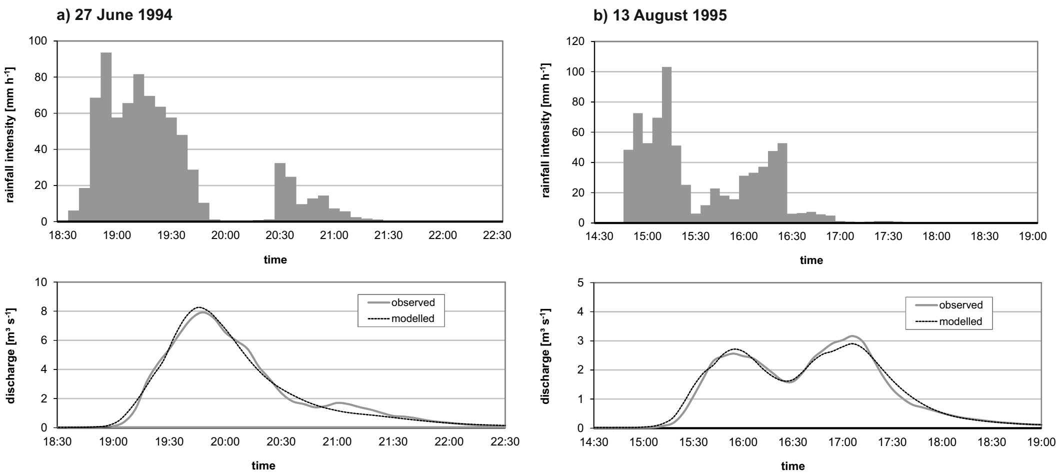

Figure 11. Rainfall intensity as well as observed and modeled hydrograph at gauge Menzingen in the Weiherbach catchment for the heavy storm events on **(a)** 27 June 1994 and **(b)** 13 August 1995.

HESSD
12, 3527–3592, 2015

Predicting land use and soil controls on erosion and sediment redistribution

U. Scherer and E. Zehe

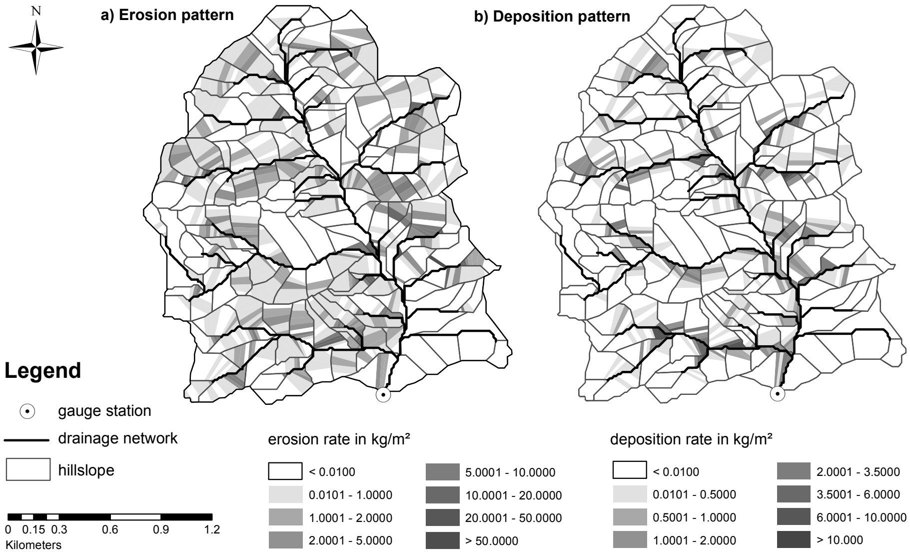

Figure 12. Visualization of modelled cumulative erosion and deposition rates in kg m^{-2} for the largest observed erosion event in the Weiherbach catchment on 27 June 1994.

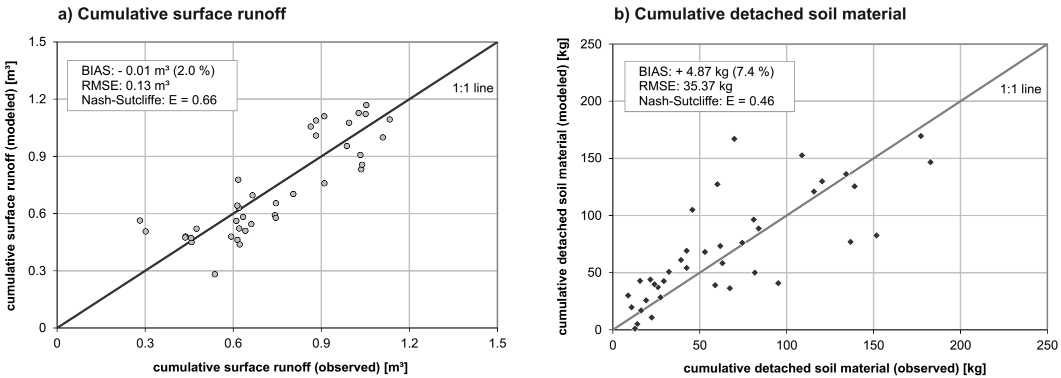

Figure 13. Comparison of **(a)** observed and modelled cumulative surface runoff and **(b)** cumulative detached soil material of 39 rainfall simulation experiments using predicted values for the model parameters macroporosity factor and erosion resistance. Where BIAS is systematic error, RMSE root mean square error and *E* model efficiency (Nash and Sutcliffe, 1970).

HESSD
12, 3527–3592, 2015